



## Towards a semi-asynchronous method for hydrological modeling in climate change studies

Frédéric Talbot<sup>1</sup>, Simon Ricard<sup>3</sup>, Jean-Daniel Sylvain<sup>2</sup>, Guillaume Drolet<sup>2</sup>, Annie Poulin<sup>1</sup>, Jean-Luc Martel<sup>1</sup>, Richard Arsenault<sup>1</sup>

5 <sup>1</sup> Hydrology, Climate and Climate Change Laboratory, École de technologie supérieure, Université du Québec, Montréal, H3C 1K3, Canada

<sup>2</sup> Direction de la recherche forestière, Ministère des Ressources naturelles et des Forêts, Québec, G1P 3W8, Canada

<sup>3</sup> Sciences and Engineering, Université Laval, Québec, G1V 0A6, Canada

*Correspondence to:* Frédéric Talbot (frederic.talbot.2@ens.etsmtl.ca)

10 **Abstract.** This study assesses the performance of the asynchronous approach used in hydrological modeling, which stands apart from the conventional approach by calibrating streamflow distributions without relying on meteorological observations. The focus is on comparing the two methods within the context of climate change impact studies, particularly in their ability to simulate key hydroclimatic processes across catchments. The analysis, conducted across multiple catchments, including a detailed case study of the Matane catchment in Southern Quebec, explores the potential of the asynchronous  
15 method as a viable alternative for future hydrological modeling. By eliminating the dependency on meteorological observations, the asynchronous approach offers potential advantages in regions with limited or unreliable observational data, providing a more flexible tool for climate change impact assessments.

The results reveal that while the asynchronous method effectively captures the overall distribution of streamflow and preserves extreme values, it faces significant challenges in accurately representing the timing of hydrological events,  
20 particularly those related to snowmelt. This issue stems, in part, from the method's decision to work directly with the biases present in raw climate model outputs, without adjusting for the timing discrepancies in meteorological inputs. Consequently, the asynchronous approach inherits these biases, leading to timing inconsistencies and increased variability across different climate models, which raises concerns about the method's ability to reliably simulate critical hydroclimatic variables under future climate scenarios. In contrast, the conventional method, which incorporates bias correction, demonstrates greater  
25 reliability in capturing the timing and magnitude of streamflow events, making it a more robust tool for most hydrological applications.

The study also highlights the concept of equifinality, where different methods achieve similar outcomes through potentially flawed mechanisms, particularly in the case of the asynchronous method. Despite projecting changes in hydroclimatic variables similar to those of the conventional method, the asynchronous approach may do so for reasons that are not  
30 hydrologically sound, particularly in snow-dominated catchments.

While the asynchronous method shows promise in preserving streamflow extremes, its current implementation requires further refinement to improve its accuracy and reliability, particularly in how it simulates the timing of seasonal dynamics. However, as climate model simulations continue to improve and their biases are progressively reduced, the asynchronous



approach is poised to benefit significantly, enhancing its potential for more accurate and reliable future hydrological  
35 projections. The conventional method remains the preferred choice for applications requiring hydrological simulations, but  
future research should focus on developing semi-asynchronous approaches that combine the asynchronous method's strength  
in preserving extremes with the conventional method's ability to handle event-specific timing.

## 1 Introduction

Climate change is one of the most significant challenges of our time, with profound implications for the Earth's hydrological  
40 systems. Alterations in temperature and precipitation regimes affect water availability and the timing of hydrological events.  
Understanding these impacts is crucial for effective water resource management and decision-making (Arsenault et al., 2013;  
Calvin et al., 2023). Accurate climate change studies are essential for developing strategies to mitigate and adapt to these  
changes, ensuring the sustainability of natural resources and the resilience of human and ecological systems (Milly et al.,  
2005; Sivakumar, 2011).

45 The complex dynamics of watersheds require hydrological models capable of precisely simulating both surface and  
subsurface processes (Farjad et al., 2016; T. W. Chu and A. Shirmohammadi, 2004). Accurate depiction of these processes  
within hydrological models is essential for assessing the impacts of climate change (Kour *et al.*, 2016; Talbot *et al.*, 2024b).  
Physically based and spatially distributed hydrological models, such as the Water Balance Simulation Model (WaSiM)  
(Schulla, 2021), are particularly valuable due to their detailed representation of key processes including surface runoff,  
50 groundwater recharge, interflow, and baseflow. These models enable accurately simulating hydroclimatic variables, which  
are essential for understanding the physical processes driving water flow and distribution in a catchment (Bormann and  
Elfert, 2010; Förster et al., 2017, 2018; Jasper et al., 2006; Natkhin et al., 2012). The use of physically based models like  
WaSiM, which capture local heterogeneity and finer-scale processes, provides a robust framework for evaluating climate  
change impacts on hydrology (Devia et al., 2015; Ludwig et al., 2009; Poulin et al., 2011) and supports stakeholders in  
55 making decisions that are both data-driven and aligned with strategic goals.

The conventional method for evaluating climate change impacts on hydrology involves a multi-step modeling chain. This  
method typically starts with the calibration of a hydrological model using observed meteorological data. Subsequently, raw  
climate model outputs are corrected using techniques such as quantile mapping (Jakob Themeßl et al., 2011; Mpelasoka and  
Chiew, 2009) to reduce potential biases in the observed data. The calibrated hydrological model is then driven by these bias-  
60 corrected climate data to simulate hydrological processes over both a reference and a future period. By comparing the  
differences between these two periods, the method estimates the potential effects of climate change on hydroclimatic  
variables, enabling a clearer understanding of how projected climate changes will influence key hydrological processes.

While widely used, conventional methods have several limitations. Bias correction can disrupt the physical consistency  
between simulated climate variables and affect long-term climate change signals (Chen et al., 2021; Lee et al., 2019).  
65 Advanced techniques, such as multivariate quantile mapping bias correction (MBCn) (Cannon, 2018), have been developed



to address some of these issues, offering a more nuanced approach preserving the inter-variable relationships essential for reliable hydrological modeling.

Chen et al. (2021) further highlights the challenges of maintaining the integrity of climate signals due to the nonstationarity of biases in climate model outputs over time. Their study, which compares pre-processing bias correction of climate model outputs with post-processing corrections applied directly to hydrological model outputs, reveals that while both approaches can significantly reduce biases, they also introduce uncertainties, particularly when dealing with sharp seasonal gradients in correction factors. Despite these challenges, they recommend pre-processing as the preferred method for climate impact studies. Additionally, conventional methods rely on high-quality meteorological observations, which are often unavailable in many regions (Ricard et al., 2023).

New approaches like asynchronous method have been proposed to address some of these challenges (Ricard et al., 2019, 2020; Ricard et al., 2023; Valencia Giraldo et al., 2023). This framework avoids the need for bias correction by adapting the hydrological model calibration process to directly use raw climate model projections data. This allows to conduct climate change studies without relying on observed meteorological data. Because the sequence of climatic events within climate model simulations is different from the historical observations, one cannot use the correlation between observed and simulated streamflow during the calibration process. Instead, the asynchronous method focuses on calibrating proxies for the distribution of streamflow rather than reproducing historical time series. Given that most of climate change impact studies assess the projected change in statistical properties between a reference and a future period (Piani et al., 2010), the need for accurate temporal correlation may become less critical (Ricard et al., 2019).

Given its potential advantages, a key question is whether the asynchronous method sacrifices the integrity of hydroclimatic variables in its pursuit of accurately reproducing streamflow distributions. To address this, this study compares hydroclimatic variables simulated by a physically based hydrological model (WaSiM) across 10 catchments, using both the conventional and asynchronous methods for climate change impact assessments. By examining the outcomes of both methods, this research aims to evaluate the asynchronous method's capacity to reliably simulate hydrological processes within catchments. The results highlight the strengths and limitations of the asynchronous framework, offering valuable insights for advancing hydrological modeling in climate change studies.

## 2 Methods and data

### 2.1 Study area

The study focuses on a selection of forested catchments in Southern Quebec, Canada, chosen for their varied sizes and hydrological characteristics. These catchments range in area from 549 km<sup>2</sup> to 1910 km<sup>2</sup> (Table 1), providing a diverse representation of the region's physiographic and climatic conditions (Fig. 1). This subset was selected from catchments previously studied (Talbot et al., 2024a, b), where we have extensive knowledge of their behavior and a well-established baseline for comparison. These catchments are well-suited for hydrological modeling with WaSiM, as their natural



hydrological processes remain largely intact and are minimally influenced by human-made structures such as dams. The availability of comprehensive streamflow data further supports their suitability for this study.

100 The region experiences a humid continental climate, with significant seasonal variation characterized by cold, snowy winters and warm, rainy summers. The Köppen-Geiger Climate Classification designates most of this region as Dfb (Humid Continental Mild Summer Wet All Year), with a smaller northern part classified as Dfc (Subarctic with Cool Summers and Year-round Precipitation) (Beck et al., 2018).

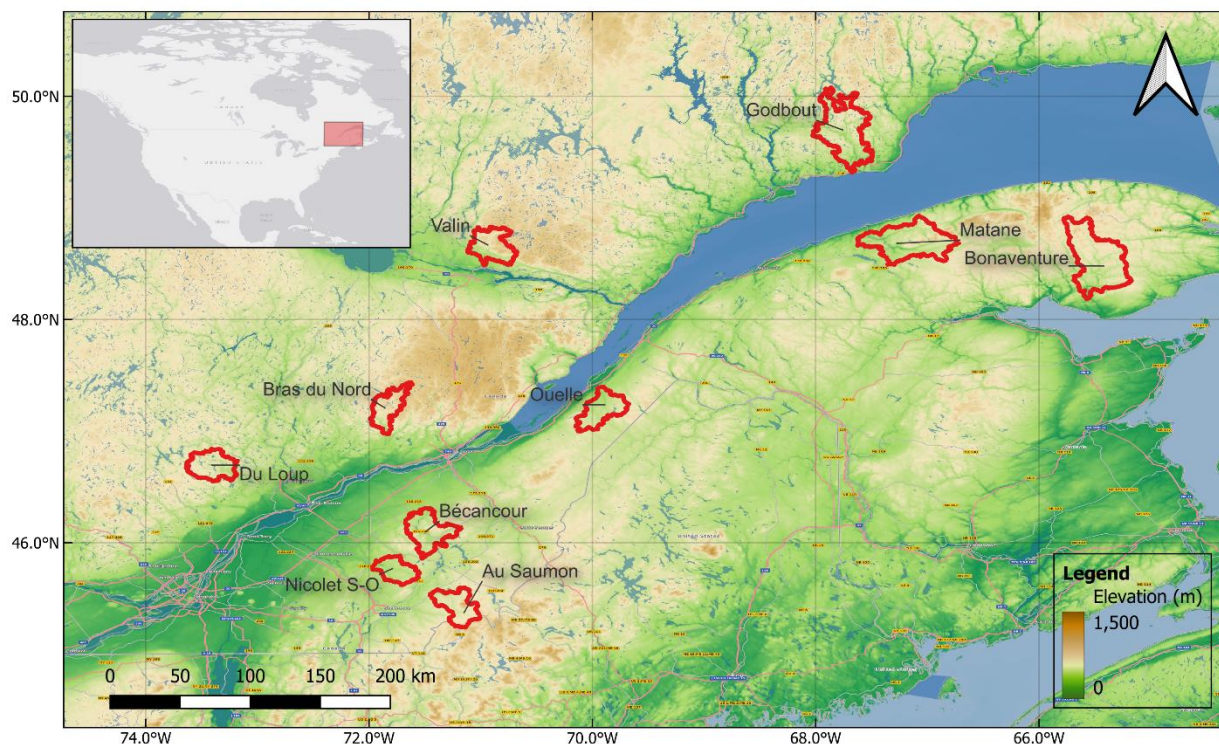
105 Climatic conditions show marked seasonal variations. Winters, extending from December to February, are cold with significant snowfall, contributing to the snowpack that influences spring runoff. Average temperatures during these months frequently drop below freezing, and snow depths can accumulate substantially, impacting streamflow upon melting.

110 Summers, from June to August, are characterized by warm temperatures and increased rainfall (Fig. 6). The transitional seasons of spring (March to May) and autumn (September to November) exhibit moderate temperatures and variable precipitation, playing a significant role in the hydrological cycle by contributing to groundwater recharge and streamflow variability.

**Table 1. Physical and meteorological characteristics of the selected catchments in Southern Quebec.**

Catchments	Area (km <sup>2</sup> )	Mean Elevation (m)	Most Common Soil Type	Most Common Land Use	Annual Rainfall <sup>a</sup> (mm)	Annual Snowfall <sup>a</sup> (mm)	Annual Runoff (mm)
Bonaventure	1910	356	Sandy Loam	Coniferous forest	753	446	675
Matane	1650	284	Sandy Loam	Mixed forest	789	480	722
Ouelle	795	315	Sandy Loam	Mixed forest	826	424	604
Bécancour	919	305	Sandy Loam	Deciduous forest	1011	389	743
Nicolet S-O	549	259	Sandy Loam	Cropland	1057	341	719
Au Saumon	738	465	Loam	Deciduous forest	935	446	810
Bras du Nord	642	511	Sandy Loam	Mixed forest	1034	444	952
Du Loup	774	381	Sandy Loam	Mixed forest	795	355	504
Valin	746	441	Sandy Loam	Mixed forest	922	436	988
Godbout	1570	302	Sandy Loam	Coniferous forest	732	434	822

<sup>a</sup> Derived from WaSiM simulations for the period 1981 to 2020, using ERA5 data as input.



115 **Figure 1. Locations of the selected catchments within Southern Quebec, outlined in red. The inset map provides the location of the study area within North America.**

## 2.2 Data

### 2.2.1 Hydrometeorological

This study utilizes daily total precipitation and mean temperature data from the ECMWF Reanalysis v5 (ERA5) (Hersbach et al., 2020) for the period 1981 to 2020. ERA5 was chosen due to its advanced features over previous reanalysis datasets, such as finer spatial resolution, hourly time step, and a more sophisticated data assimilation system that incorporates a wider range of observational inputs (Tarek et al., 2020). These features make ERA5 a suitable reference dataset for hydrological modeling, as demonstrated in Tarek *et al.* (2020), where ERA5-based hydrological simulations performed equivalently to observational data in most regions, including our study area. Additionally, ERA5 showed reduced biases in temperature and precipitation compared to the ERA-Interim dataset, further justifying its use as a reliable and accurate source of climate data.

120

125 Streamflow data was sourced from the *Hydroclimatic Atlas of Southern Québec* (MDDELCC, 2022), covering the period from 1981 to 2010. This dataset provides daily measurements, though some catchments have minor gaps, primarily during winter months due to ice cover and ice jams. These periods were excluded from model calibration and analyses to maintain data accuracy.



### 2.2.2 Elevation

130 A hydrologically conditioned digital surface model (DEM) was derived from the NASA Shuttle Radar Topography Mission version 3.0 Global 1 arc second (SRTMGL1). Hydrological corrections ensured accurate representation of hydrological networks, with adjustments made using SAGA GIS software (Conrad et al., 2015). Basin delineation and analysis were conducted using QGIS and Tanalys software (Schulla, 2021) to extract essential topographic information for hydrological modeling.

### 135 2.2.3 Soil type

Soil data was sourced from the SIIGSOL 100 meters database, which provides detailed descriptions of sand, clay, and silt proportions within the soil profile (Ministère des Ressources Naturelles et des Forêts, 2022; Sylvain et al., 2021). These proportions were converted to soil texture classes based on the USDA classification system (Soil Survey Division Staff, 2017). Soil hydraulic properties were imputed from established relationships between soil texture classes and hydraulic parameters. Elevation data was used to account for soil depth variability, classifying raster cells into deep, normal, and shallow categories based on their relative elevation as described in (Talbot et al., 2024a).

### 2.2.4 Land use

Land use data was obtained from the 2015 North American Land Change Monitoring System (NALCMS) 30 meters dataset. This data was resampled using the nearest neighbor method to create land use maps, significantly impacting hydrological parameters such as root distribution, vegetation cover fraction (VCF), roughness length (Z0), and albedo. These parameters influence processes like evapotranspiration, runoff, and infiltration (2015 Land Cover of North America at 30 meters, 2023; Latifovic et al., 2012).

### 2.2.5 Climate models

Projected daily temperature and precipitation data were sourced from the Coupled Model Intercomparison Project Phase 6 (CMIP6) (O'Neill et al., 2016) for both the reference period (1981-2010) and future period (2070-2099). These datasets were accessed and processed through the PAVICS-Hydro platform (Arsenault et al., 2023). The Shared Socioeconomic Pathway 5-8.5 (SSP5-8.5) scenario, which projects very high greenhouse gas emissions, was used to simulate future conditions (Calvin et al., 2023). To address uncertainties related to climate model selection, an ensemble of 18 climate models was employed as it was previously shown that, to ensure robustness, using multiple climate models is required (Arsenault et al., 2020; Lucas-Picher et al., 2021; Minville et al., 2008; Tarek et al., 2021). This ensemble approach ensures a more robust representation of potential climate outcomes by capturing a range of possible future scenarios.



## 2.3 Hydrological modelling

### 2.3.1 Hydrological model

160 WaSiM is a physically based, spatially distributed hydrological model designed to simulate water flow processes in catchments. It integrates a comprehensive suite of sub-models to capture key hydrological processes, including surface runoff, groundwater recharge, interflow, and baseflow, within a deterministic framework (Schulla, 2021).

In this study, WaSiM was configured with a spatial resolution of 1000 meters and a temporal resolution of 24 hours. This setup allows for detailed spatial analysis while maintaining computational efficiency. The chosen spatial resolution ensures that the heterogeneity of the landscape is adequately captured, and the daily time step allows for accurate simulation of hydrological processes over time.

165 WaSiM employs the Richards equation and the Van Genuchten parameters for simulating water flow in the unsaturated zone (van Genuchten, 1980; Richards, 1931). This equation provides a physically based representation of hydraulic head gradients and soil moisture dynamics, incorporating detailed soil physical properties. Groundwater flow is calculated conceptually within the unsaturated zone model.

### 170 2.3.2 Conventional method

The framework used to calibrate and validate the effectiveness of the conventional method rely on the split sample test (SST) approach, which is widely recognized for its effectiveness in evaluating model performance. This approach involves dividing the data into separate calibration and validation periods, allowing for an assessment of the model's ability to generalize beyond the calibration conditions.

175 For this method, historical data from ERA5 were used for both calibration and validation. The calibration period spanned from 2000 to 2009, during which simulations were performed over a 15-year period (1995 to 2009), discarding the first 5 years to stabilize the initial conditions of the model. The validation period was set from 1990 to 1999, following the same approach of conducting simulations over a 15-year period (1985 to 1999) and discarding the initial 5 years.

180 A set of 17 parameters (Table 2) was selected for calibration based on model documentation and the configuration used in Talbot *et al.* (2024a). Table 2 was taken from Talbot *et al.* (2024a).



**Table 2. Calibration parameters for the hydrological model WaSiM.**

No.	Code	Description	Sub-Model	Range
1	$k_D$	Storage coefficient for surface runoff (h)	Unsaturated zone	[1, 25]
2	$k_H$	Storage coefficient for interflow (h)	Unsaturated zone	[1, 25]
3	$d_r$	Drainage density for interflow ( $m^{-1}$ )	Unsaturated zone	[1, 50]
4	$QD_{Snow}$	Fraction of surface runoff on snow melt	Unsaturated zone	[0.1, 1]
5	$c_0$	Degree-Day factor ( $mm\ ^\circ C^{-1}\ d^{-1}$ )	Snow	[0, 3]
6	$T_0$	Temperature limit for snow melt ( $^\circ C$ )	Snow	[-4, 4]
7	$T_{R/S}$	Transition temperature snow/rain ( $^\circ C$ )	Snow	[-4, 4]
8	$C_{WH}$	Water storage capacity of snow	Snow	[0.1, 0.3]
9	$C_{rfr}$	Coefficient for refreezing	Snow	[0.1, 1]
10	$f_{i,summer}$	Summer correction factors for PET	Evapotranspiration	[0.1, 2]
11	$f_{i,fall}$	Fall correction factors for PET	Evapotranspiration	[0.1, 2]
12	$f_{i,winter}$	Winter correction factors for PET	Evapotranspiration	[0.1, 2]
13	$f_{i,spring}$	Spring correction factors for PET	Evapotranspiration	[0.1, 2]
14	$K_{rec}$	Recession constant for hydraulic conductivity	Soil table	[0.1, 0.99]
15	$d_z^a$	Soil layer thickness	Soil table	[0.8, 1.4]
16	KB	Storage coefficient for base flow (m)	Unsaturated zone	[0.1, 8]
17	Q0	Scaling factor for base flow ( $mm\ h^{-1}$ )	Unsaturated zone	[0.1, 5]

<sup>a</sup> Calibration coefficient, ranging from 0.8 to 1.4, is applied to adjust the total soil depth, which is predetermined to be 8 meters for shallow, 14 meters for normal, and 20 meters for deep soil conditions.

190 These parameters were optimized based on a single objective function through the Dynamically Dimensioned Search (DDS) algorithm, developed by Tolson and Shoemaker (2007). This algorithm was chosen for its efficiency in handling complex optimization problems for compute-intensive hydrological models, as recommended by Arsenault *et al.* (2014).

The objective function used for calibration was the Kling Gupta-Efficiency (KGE) (Kling *et al.*, 2012). The KGE metric provides a balanced evaluation of model performance by considering simultaneously correlation, variability, and bias in the simulated streamflow relative to observed streamflow.

The KGE is computed using Eq. (1):

$$195 \quad KGE = 1 - \sqrt{(r - 1)^2 + \left(\frac{\sigma_{sim}/\mu_{sim}}{\sigma_{obs}/\mu_{obs}} - 1\right)^2 + \left(\frac{\mu_{sim}}{\mu_{obs}} - 1\right)^2}, \quad (1)$$

where  $r$  is the correlation coefficient between simulated and observed streamflow,  $\sigma_{sim}$  is the standard deviation of simulated streamflow,  $\sigma_{obs}$  is the standard deviation of observed streamflow,  $\mu_{sim}$  is the mean of the simulated streamflow, and  $\mu_{obs}$  is the mean of the observed streamflow.





200 A KGE value of 1 indicates a perfect match between the simulated and observed streamflow, reflecting ideal performance across all three components: correlation, variability, and bias.

To address biases in the climate model simulations, the Multivariate Bias Correction algorithm (MBCn) of Cannon (2018) was utilized. This method corrects biases in meteorological data while accounting for spatiotemporal interdependencies between variables and preserving changes in quantiles between the reference (1981-2010) and future (2070-2099) periods. The bias correction was applied to daily total precipitation and daily mean temperature using ERA5 data as the reference  
205 over the period 1981-2010 and was used to correct the climate models data for both the reference (1981-2010) and future periods (2070-2099).

For the conventional method, climate change hydrological simulations were performed using the bias-corrected climate models data. Simulations were conducted for each climate model over the reference and future periods using the calibrated hydrological model for each catchment.

### 210 2.3.3 Asynchronous method

The primary objective of the asynchronous method is to conduct climate change studies without relying on observed meteorological data (Ricard et al., 2019, 2020; Ricard et al., 2023) and eliminate the need for bias-correction of climate variables. Instead, the calibration is performed using raw climate model data and observed streamflow, integrating the bias-correction in the calibration step. A significant challenge in this approach is the lack of synchronization between the timings  
215 of observed streamflows and those of raw climate model outputs (Ricard et al., 2019), as climate models are not temporally aligned with actual past events. This requires a departure from the conventional calibration framework, which aims to optimize the synchronicity and amplitude of streamflow.

To overcome this obstacle, the objective function optimizes the distribution of observed streamflow over an extended period rather than individual streamflow observations. This approach ensures the hydrological model effectively captures the streamflow distribution, rather than day-to-day natural variability.  
220

Given the calibration objectives of the asynchronous method, the observed streamflow data from 1984 to 2009 was sorted and used to establish a reference distribution of streamflow. This sorted distribution provided a consistent target for both the calibration and validation of the hydrological model. In the context of the asynchronous method, where direct temporal alignment between climate model outputs and observed streamflow is not maintained, relying on the same observed  
225 distribution for both calibration and validation ensures that the model is evaluated against a stable and representative reference. Therefore, a 25-year period (1984-2009) was used for both calibration and validation, as it captures a broad range of hydrological conditions, minimizes the influence of short-term climate variability, and mitigates biases that could arise from using shorter time frames. A key hypothesis underlying this approach is the assumption of stationarity—that the hydrological model, with fixed parameters optimized during calibration, will continue to produce reasonable streamflow  
230 simulations under future climate conditions. This assumes that despite changing climatic conditions, the model will adequately respond to future scenarios as it did to past conditions. However, if future climate changes introduce conditions



outside the model's calibrated range, such as new snow patterns or shifts in seasonal dynamics, the model's performance could be compromised.

235 The calibration and validation periods are separated based on the total yearly precipitation from October to September. This separation ensures an equal distribution of wet and dry years between both periods. Simulations were performed for the years 1984 to 2011, with the first two years discarded to allow for initial model stabilization. Out of the 26 years of simulations, 13 years were used for calibration, selected based on total yearly precipitation, while all 26 years were utilized for model validation.

240 To address biases in simulated streamflow resulting from biases in precipitation and temperature in the raw climate data, the simulated streamflow was adjusted by multiplying it by a factor equal to the ratio of the mean observed streamflow  $Q_{obs}$  to the mean simulated streamflow  $Q_{sim}$ . This adjustment was applied only during the calibration process and not during the reference or future periods simulations. It ensures that the mean simulated streamflow matches the mean observed streamflow, effectively removing bias. This means the simulated absolute streamflow values cannot be directly compared with observations, but changes between the reference and future period can be analyzed.

245 The Root Mean Square Error (RMSE) was employed as the objective function:

$$RMSE = \sqrt{\frac{1}{n} \sum_{i=1}^n (Q_{sim_i} - Q_{obs_i})^2}, \quad (2)$$

where  $Q_{sim}$  represents the sorted simulated streamflow (mm),  $Q_{obs}$  represents the sorted observed streamflow (mm), and  $n$  is the number of simulated streamflow values.

250 Each climate model was calibrated for each catchment, resulting in a total of 180 calibration parameter sets (18 climate models x 10 catchments). In contrast, the conventional method involves 10 calibration parameter sets (one per catchment) which is then applied to all climate models and their bias-corrected outputs. Consequently, the asynchronous method is considerably more computationally intensive than the conventional method in terms of parameter calibration.

The calibration framework for the asynchronous method is similar to that of the conventional method. It involves 1000 trials, uses the same 17 calibration parameters (Table 2), and employs DDS optimization algorithm.

255 For the asynchronous method, climate change simulations were conducted using the calibrated model for each catchment and each projected climate model, but without relying on historical event timing. Raw projected climate data were utilized to perform simulations over both the reference and future periods.

## 2.4 Comparative analysis

260 The comparative analysis in this study is designed to evaluate the performance of the conventional and asynchronous methods in simulating hydrological processes under both current and future climate conditions. To ensure a fair and unbiased comparison, both methods employed the same WaSiM configuration, including identical calibration parameters, the number of evaluations, and the optimization algorithm. This was performed to ensure minimal calibration bias and to isolate the differences attributable solely to the methodological framework of each approach.



The first step in the comparative analysis involves assessing the calibration and validation performance of each method. Streamflow simulations were evaluated using the KGE for the conventional method and the RMSE of the sorted simulated and observed streamflow for the asynchronous method. These metrics were selected to highlight each method's strengths in different aspects of streamflow simulation—KGE for overall model performance and RMSE for the accuracy of flow distribution.

Beyond streamflow, we also examine the relationships between various hydroclimatic variables, such as groundwater recharge, surface runoff, soil moisture, and snow water equivalent (SWE). By comparing the simulated values from both methods, the analysis seeks to understand how well each method captures the interactions between these variables. This serves to evaluate the internal consistency of the models and assess their ability to realistically simulate the physical processes within the catchments.

The analysis extends to a comparison of the projected changes in hydroclimatic variables between the reference period (1981–2010) and the future period (2070–2099). The magnitude and direction of these changes are assessed to determine how each method projects the impact of climate change on the catchments. This includes examining variables such as changes in snowmelt dynamics, and the consequent effects on streamflow, surface runoff and groundwater recharge.

A detailed spatial analysis is conducted to evaluate the distribution of key variables, such as soil moisture and groundwater recharge, across the catchments. The comparative analysis employs several criteria to determine which method is more effective. These include the accuracy of streamflow simulation (both in terms of overall distribution and event timing), the internal consistency of hydroclimatic variable relationships and the realism of spatial distributions and projected changes under future climate scenarios. The method that consistently demonstrates superior performance across these criteria is considered more reliable for future hydrological modeling and climate impact assessments.

### 3 Results

#### 3.1 Streamflow representation performance

For the conventional method, streamflow representation performance was assessed using the KGE metric for each catchment during both the calibration and validation periods.

During calibration, the conventional method achieves KGE values ranging from 0.817 to 0.906, with a mean of 0.863. Similarly, for the validation period, the KGE values ranged from 0.778 to 0.906, with a mean of 0.842. These results indicate that the conventional method maintains a consistent performance in simulating streamflow across different catchments. Detailed KGE results for each catchment are provided in the Appendix A (Table A1).

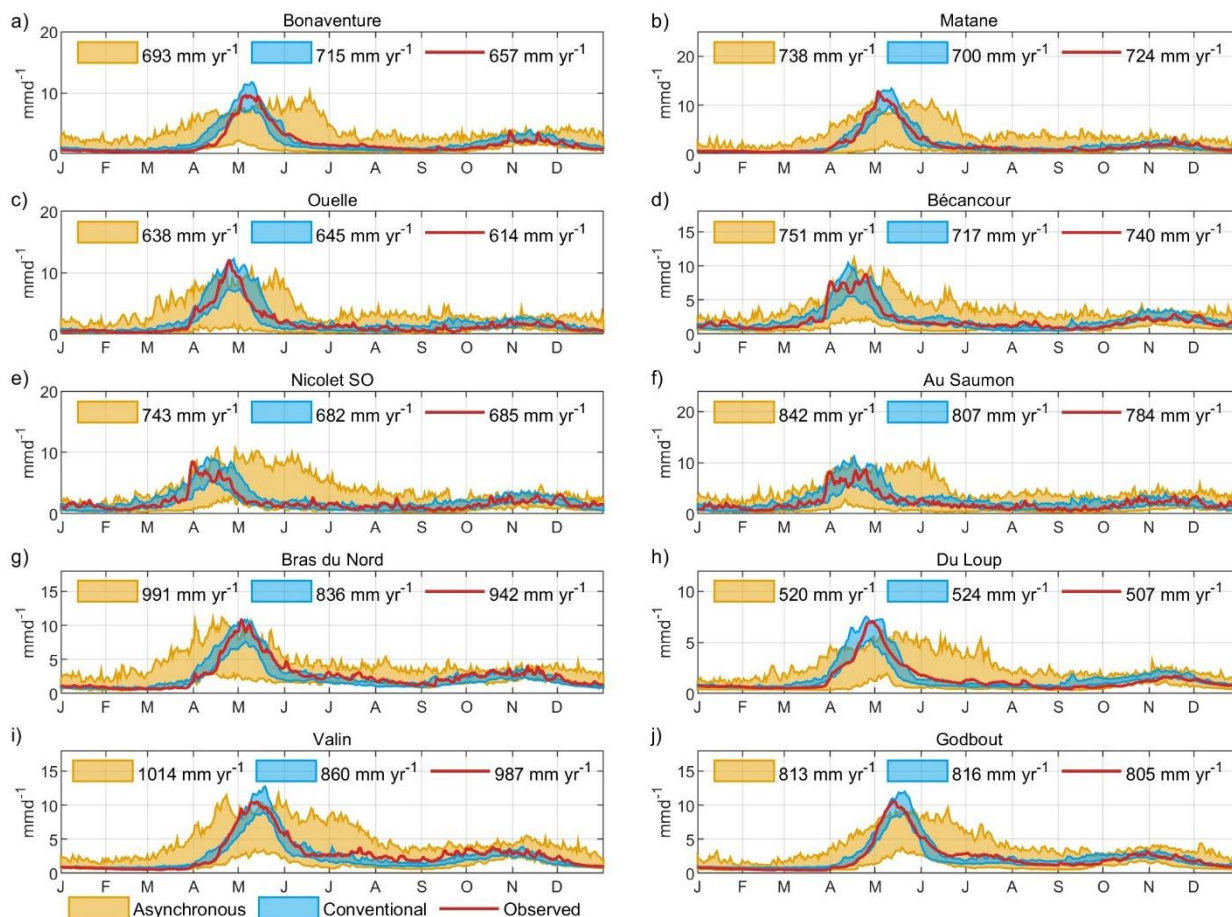
For the asynchronous method, the RMSE was used to evaluate streamflow representation performance during both the calibration and validation periods. During calibration, the RMSE values exhibited a mean of 0.121 mm d<sup>-1</sup> with a mean standard deviation between climate models of 0.031 mm d<sup>-1</sup>. In the validation period, the RMSE values demonstrated similar



295 patterns, with a mean of  $0.179 \text{ mm d}^{-1}$  and a standard deviation of  $0.057 \text{ mm d}^{-1}$ . Detailed RMSE values are available in the Appendix A (Table A2).

Figure 2 presents hydrographs of streamflow for both methods during the reference period across the ten catchments, along with observed streamflow for the same period. The asynchronous method shows greater variability between climate models, especially in the timing of peak flows, which often fails to align with the observed data, as expected. This variability suggests that the timing of streamflow events in the asynchronous method is highly sensitive to the specific climate model employed. For instance, in the Matane catchment, the observed and conventional method peak flow occurs at the beginning of May, while the asynchronous method shows a broader range of peak flow timings, extending from early May to late June. This discrepancy might be attributed to challenges in accurately simulating snowmelt processes with the asynchronous method, which are crucial for generating high flows in the study region. Furthermore, in the same catchment, the asynchronous method overestimates summer flows compared to the observed data, indicating potential difficulties in capturing the seasonal dynamics of low-flow periods. Conversely, the conventional method accurately reproduces the annual observed streamflow variability, demonstrating its strength in capturing the timing and magnitude of hydrological events.

305 Despite these differences, the asynchronous method outperforms the conventional method in terms of annual volume accuracy in 8 out of 10 catchments (Fig. 2). This enhanced accuracy can be attributed to the scaling adjustments applied during the calibration period. In the asynchronous method, streamflow is adjusted by multiplying them by a scaling factor to correct biases between simulated and observed means, effectively minimizing the difference between overall volume in simulated and observed streamflow. However, the inability of the asynchronous simulations to replicate the precise timing of streamflow events raises concerns about its representation of underlying hydroclimatic variables, which may impact the model's broader predictive accuracy.



315

**Figure 2. Seasonal streamflow comparison between the asynchronous and conventional methods and observed data across ten catchments during the reference period (1981–2010). The panels (a-j) represent the catchments of Bonaventure, Matane, Ouelle, Bécancour, Nicolet SO, Au Saumon, Bras du Nord, Du Loup, Valin, and Godbout, respectively. The colored bands indicate the range of daily streamflow simulated by the asynchronous method (yellow) and conventional method (blue) alongside the observed streamflow (red line).**

320

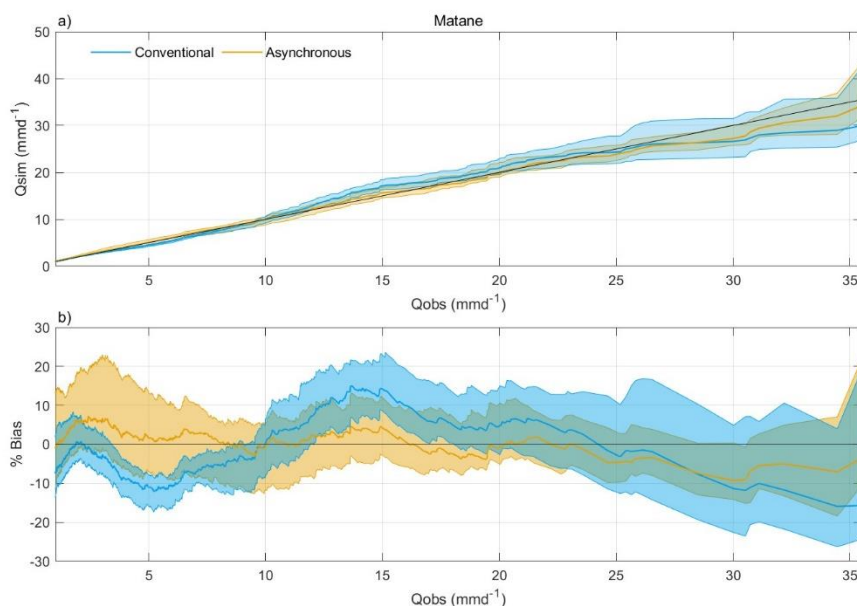
Figure 3 shows the relationship between the sorted streamflow distribution and percentage bias for simulated and observed values using conventional and asynchronous methods during the reference period (1981–2010) for the Matane catchment. Climate models using the conventional method exhibit broader dispersion compared to the asynchronous method. Moreover, the asynchronous method demonstrates a better ability to capture extreme streamflow events, as indicated by its lower percentage bias across a range of streamflow conditions. This suggests that the asynchronous method is more effective in predicting extreme flows and capturing the overall distribution of streamflow, likely due to its calibration focus on streamflow distribution rather than the precise timing of hydrological events.

325



330 While these results are specific to the Matane catchment, similar patterns are observed across all catchments studied (Fig. B1 to Fig. B9). This consistency highlights the asynchronous method's strength in capturing the full range of potential streamflow conditions across diverse hydrological settings, particularly in representing extremes.

In contrast, the conventional method excels at capturing the annual fluctuations and timing of the observed streamflow but is more limited in its ability to represent extreme flows. The asynchronous method, optimized for distributions, offers a distinct advantage in this area by more accurately reflecting the range of possible streamflow values, particularly during high and low flow events.



335

**Figure 3. Performance comparison between the conventional and asynchronous methods for the Matane catchment during the reference period (1981–2010). Panel (a) displays the relationship between simulated daily streamflow ( $Q_{sim}$ ) and observed daily streamflow ( $Q_{obs}$ ) for the conventional (blue) and asynchronous (yellow) methods. The x-axis represents the observed daily streamflow, while the y-axis represents the simulated streamflow. Panel (b) shows the percentage bias between observed and simulated streamflows for both methods, with the x-axis representing the observed daily streamflow and the y-axis displaying the percentage bias relative to the observed values. The shaded regions in both panels illustrate the variability among climate models around the mean bias for each method, emphasizing the differences in how well each method simulates streamflow across the observed streamflow range.**

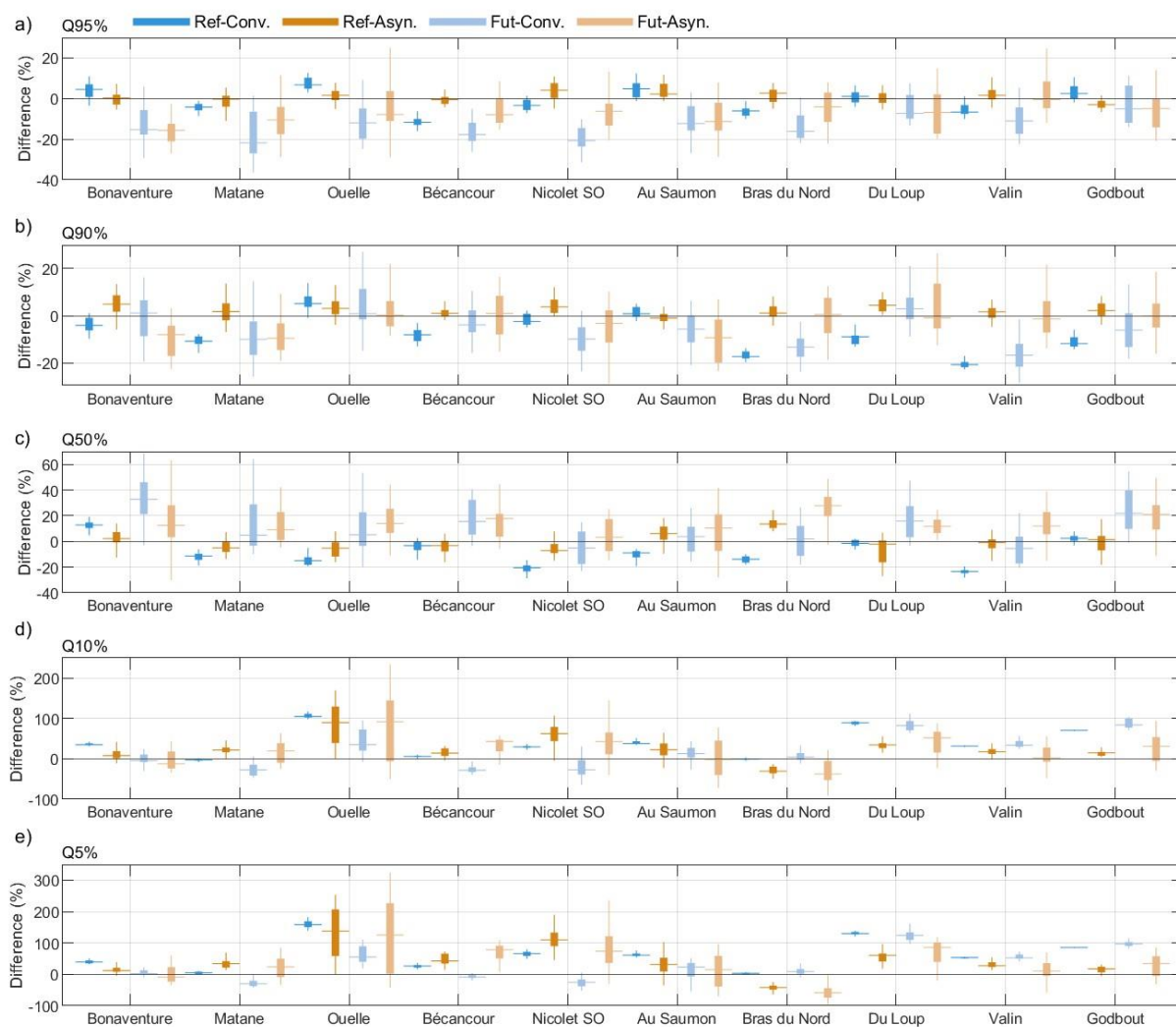
340

345 Figure 4 presents a comparative analysis of streamflow quantiles for both methods across the reference (1981–2010) and future (2070–2099) periods for all ten catchments. When comparing the observed streamflow to the reference period simulations, the asynchronous method shows a closer alignment with the observed distribution, particularly for high flows ( $Q_{95\%}$  and  $Q_{90\%}$ ), confirming its strength in capturing extreme events. However, it is important to note that the asynchronous method also exhibits a higher dispersion among climate models during the reference period, indicating greater variability in its predictions.

350 In terms of future projections, both methods demonstrate similar trends, with both projecting decreases in high flows ( $Q_{95\%}$ ) across most catchments. However, the projections for other flow quantiles, such as median ( $Q_{50\%}$ ) and low flows



(Q5% and Q10%), show mixed changes that vary depending on the catchment's geographical location. While there is a broad agreement between the methods on the direction of changes from the reference to the future period, the asynchronous method again shows a higher dispersion between climate models, especially for low flows (Q5% and Q10%). This increased variability suggests that while the asynchronous method is effective at representing the distribution of streamflow, it may introduce greater uncertainty in future projections, particularly for low-flow conditions.



360

**Figure 4. Streamflow distribution analysis for both the reference (1981–2010) and future (2070–2099) periods across 10 catchments, comparing the conventional (blue) and asynchronous (orange) methods. The figure illustrates the percentage differences in streamflow quantiles between the simulated and observed streamflow for both methods with the central line indicating the median and whiskers extending to the 25th and 75th percentiles. The panels represent the following streamflow quantiles: (a) Q95% (high flow), (b) Q90%, (c) Q50% (median flow), (d) Q10%, and (e) Q5% (low flow). For each catchment, the reference period data is shown in darker shades, while the future period projections are displayed in lighter shades. Blue represents the conventional method, and orange represents the asynchronous method.**



### 365 3.2 Hydroclimatic variables

The primary objective of this study is to compare the conventional and asynchronous methods and evaluate the ability of the asynchronous approach to accurately reproduce the physical processes within catchments. This section expands the analysis beyond streamflow to include a broader range of hydroclimatic variables, providing a more comprehensive assessment of the methods' performance.

370 Table 3 presents the annual averages for several key hydroclimatic variables—such as precipitation, snowfall, streamflow, surface runoff, interflow, actual evapotranspiration (ET<sub>a</sub>), baseflow, groundwater recharge, SWE, and soil moisture—across both the reference (1981–2010) and future (2070–2099) periods. The table also highlights the relative changes in these variables between the reference and future periods for both the conventional and asynchronous methods.

When comparing the results for the reference and future periods, both methods exhibit similar trends across most  
375 hydroclimatic variables. For instance, both methods predict an increase in precipitation and ET<sub>a</sub>, alongside a significant reduction in snowfall and SWE as a response to the anticipated warming climate.

However, notable differences arise in the representation of certain variables. One of the most significant discrepancies is observed in surface runoff. The asynchronous method predicts more than twice the amount of surface runoff compared to the conventional method, both in the reference and future periods. This substantial difference suggests that the asynchronous  
380 method may be simulating surface processes differently than the conventional method.

In terms of relative changes between the reference and future periods, both methods demonstrate similar trends across most variables, indicating agreement on the direction of change due to climate impacts. For example, both methods predict a similar reduction in snowfall (around 33% and 41%) and SWE (around 53% and 58%), reflecting the expected decrease in snow accumulation as temperatures rise. The increase in ET<sub>a</sub> (31%) is also consistent across both methods, suggesting that  
385 higher temperatures will lead to greater evapotranspiration.

390

395





400 **Table 3. Comparison of hydroclimatic variables between the reference (1981–2010) and future (2070–2099) periods for both the conventional and asynchronous methods across 10 catchments and 18 climate models. The table presents annual averages for key hydroclimatic variables, including precipitation, snowfall, streamflow, surface runoff, interflow, actual evapotranspiration (ETa), baseflow, groundwater recharge, snow water equivalent (SWE), and soil moisture. Relative changes between the reference and future periods are also provided for each method.**

Hydroclimatic Variables	Unit	Conventional			Asynchronous		
		Reference (1981-2010)	Future (2070-2099)	Relative Change	Reference (1981-2010)	Future (2070-2099)	Relative Change
Precipitation	mm yr <sup>-1</sup>	1276	1463	15%	1328	1507	13%
Snowfall	mm yr <sup>-1</sup>	409	273	-33%	362	214	-41%
Streamflow	mm yr <sup>-1</sup>	730	744	2%	771	778	1%
Surface Runoff	mm yr <sup>-1</sup>	109	77	-29%	256	199	-22%
Interflow	mm yr <sup>-1</sup>	482	530	10%	400	460	15%
ETa	mm yr <sup>-1</sup>	554	727	31%	561	733	31%
Baseflow	mm yr <sup>-1</sup>	140	137	-2%	113	117	3%
Groundwater Recharge	mm yr <sup>-1</sup>	133	139	4%	118	141	19%
SWE	mm	281	131	-53%	252	106	-58%
Soil Moisture	-	0.188	0.180	-5%	0.203	0.200	-2%

405 Figure 5 illustrates the annual variations of key hydroclimatic variables across different catchments and 18 climate models for both the reference and future periods, comparing the conventional and asynchronous methods. Several noteworthy differences emerge between the two methods, particularly in streamflow, interflow, and groundwater recharge.

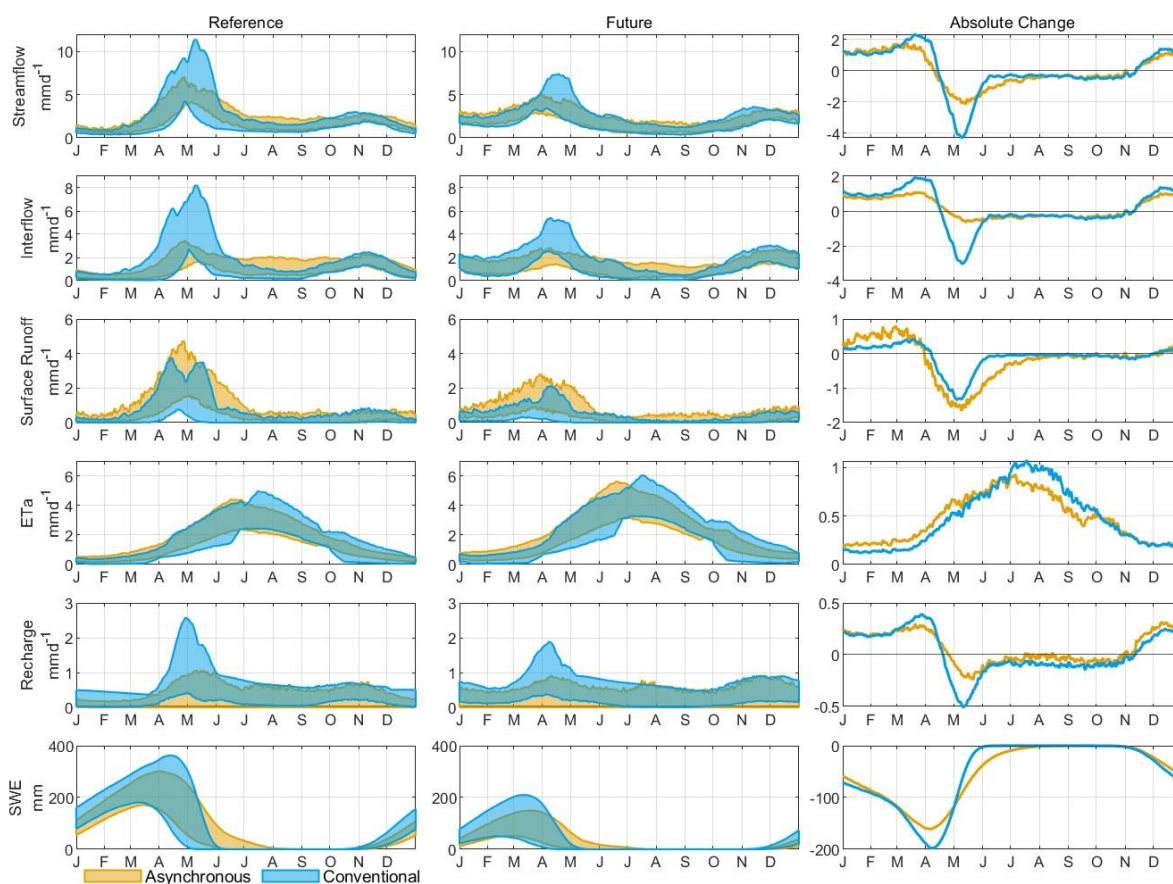
The conventional method tends to produce higher peaks for streamflow, interflow and recharge during periods of high streamflow, suggesting a more pronounced response to snowmelt and precipitation events. This method also exhibits greater variability during these high-flow periods. In contrast, the asynchronous method displays higher summer flows.

410 Both methods predict similar absolute changes in streamflow between the reference and future periods, reflecting a consistent trend across climate projections. However, the conventional method indicates a more substantial decrease in high flows in the future, which could have significant implications for water resource management, particularly in regions where peak flows are crucial for reservoir replenishment and flood control. It is thus important to assess if one of the two methods (conventional vs. asynchronous) can be considered as more reliable than the other as this could affect conclusions of many  
415 climate change impact studies.

For surface runoff, the asynchronous method consistently generates higher values compared to the conventional method across both periods. This suggests that the asynchronous method may be simulating more rapid or intense surface processes. Despite these differences in magnitude, both methods exhibit similar trends in absolute change, indicating a projected decrease in surface runoff in the future.

420 ETa results are closely aligned between the two methods. This consistency suggests that ETa projections are robust across different modeling frameworks, reinforcing confidence in these projections for water balance assessments.

Maximum SWE also shows differences between the two methods. The conventional method predicts higher SWE values, suggesting that it may simulate a more substantial accumulation of snowpack during the winter months. On the other hand, the asynchronous method demonstrates greater variability during the snowmelt period, with snowmelt extending from April to August, compared to a more concentrated snowmelt period from April to June in the conventional method. This extended snowmelt period in the asynchronous method could lead to prolonged high flows in late spring and early summer. However, it is quite unrealistic to observe snow persisting through the summer months, highlighting a significant limitation of the asynchronous method in accurately representing seasonal snow dynamics.



430 **Figure 5. Seasonal distribution of key hydroclimatic variables for the reference period (1981–2010), future period (2070–2099),**  
**435 the asynchronous method. The figure presents the monthly averages of streamflow, interflow, surface runoff, actual evapotranspiration (ETa),**  
**groundwater recharge, and snow water equivalent (SWE). The left column shows the reference period, the middle column displays**  
**the future period, and the right column illustrates the absolute changes between the two periods. The shaded areas represent the**  
**variability across the catchments.**



### 3.3 Case study

To thoroughly assess the asynchronous method's ability to accurately reproduce physical processes within a catchment, the Matane catchment, covering an area of 1650 km<sup>2</sup>, was selected as a case study. This catchment was chosen due to its strong calibration and validation performance under both methods, as well as its representative characteristics of the broader set of  
440 studied catchments.

Average monthly temperature and precipitation for the reference period (1981-2010) and the future period (2070-2099) before and after bias-correction using MBCn for the Matane catchment and the climate model ACCESS-ESM1-5 is provided as an example (Fig. 6).

In the reference period, a noticeable gap exists between the ERA5 data and the raw climate model data, with the raw climate  
445 data showing higher temperatures and increased precipitation for all months except October. The effectiveness of the bias correction is evident, as the bias-corrected climate data closely aligns with the ERA5 data, significantly reducing discrepancies in temperature and precipitation. The same bias trend is observed in the future period, where raw climate model data predicts higher temperatures and increased precipitation compared to the bias-corrected data.

Furthermore, Fig. 6 highlights the anticipated changes in precipitation and temperature between the reference and future  
450 periods. Temperatures are expected to increase significantly, with projected increases around 6 degrees Celsius across the study area. These projections are in line with the IPCC's forecasts based on SSP5-8.5, and suggest that northern latitudes will experience faster warming compared to the global average (Estrada et al., 2021). Projections consistently show an annual increase in precipitation ranging from 15 to 20%, with the most significant increases occurring between December and April, as well as in July. The anticipated increases in temperature and changes in precipitation patterns have profound implications  
455 for hydrological processes and water resource management.

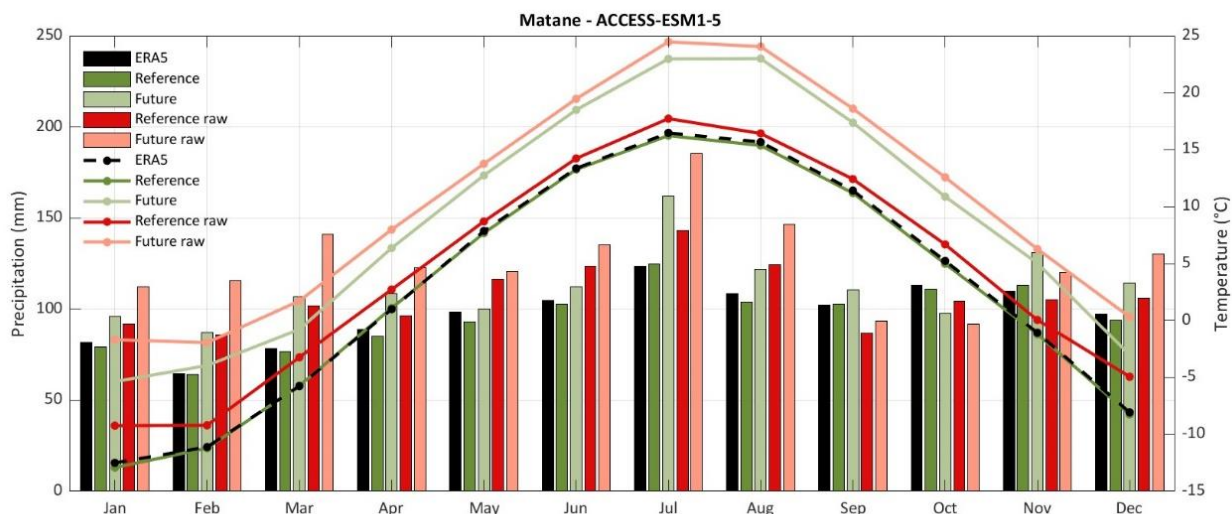


**Figure 6.** Comparison of average monthly precipitation and temperature for the Matane catchment. This figure displays the average monthly temperature and precipitation for the Matane catchment during the reference period (1981-2010) and the future period (2070-2099) under the Shared Socioeconomic Pathway 5-8.5 (SSP585) scenario. Solid lines represent average monthly temperature: green for the reference period with bias correction, light green for the future period with bias correction, red for the reference period without bias correction, and light red for the future period without bias correction. The black dashed line indicates ERA5 data for comparison. Bars represent average monthly precipitation: black for ERA5 data, green for precipitation with bias correction, and red for precipitation without bias correction. Lighter shades of the bars correspond to data for the future period, distinguishing between bias-corrected and uncorrected scenarios.

460

465

Figure 7 offers a detailed comparison of the annual variations in key hydroclimatic variables for both the reference (1981–2010) and future (2070–2099) periods, using the conventional and asynchronous methods for the Matane catchment. The figure mirrors the approach taken in Fig. 5 but focuses specifically on Matane, with the shaded areas indicating the variability across different climate models.

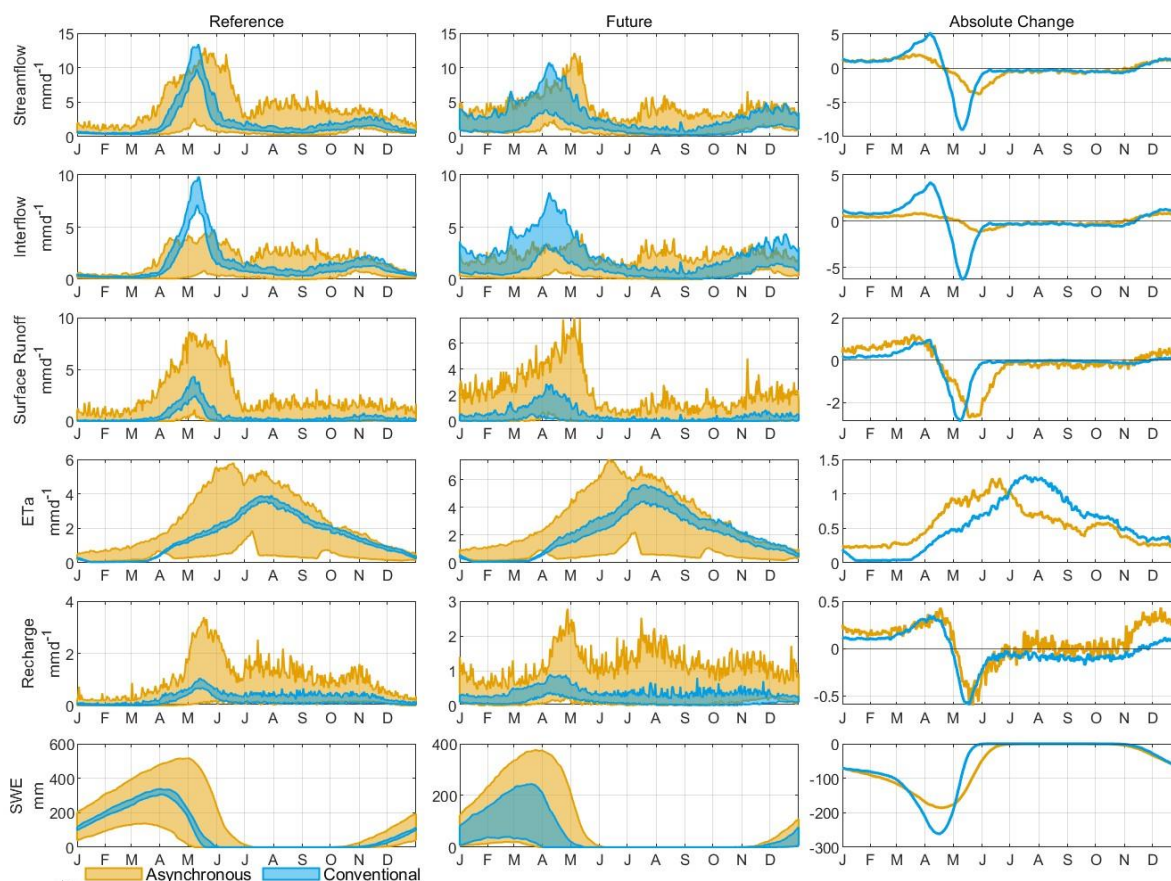
470

The trends observed in the Matane catchment largely reflect the broader findings across all catchments. For variables such as interflow, streamflow, ETa, surface runoff, and SWE, the asynchronous and conventional methods exhibit patterns that align with the general trends noted in the overall analysis. However, the asynchronous method predicts significantly more groundwater recharge in the Matane catchment compared to the conventional method.

475

A key observation from Fig. 7 is the pronounced variability between climate models when using the asynchronous method. This variability suggests that some climate models may produce an unrealistic representation of physical processes, particularly in relation to snow dynamics. For example, when examining the maximum snow water equivalent, the asynchronous method shows that the snowmelt period can start as early as April and extend as late as July, depending on the climate model. This is problematic, as it is highly unusual to have snow persist into July in the Matane region, making it unrealistic for a 30-year average to show such late snowmelt. This discrepancy raises concerns about the asynchronous method's ability to accurately simulate snow processes, a critical component of the hydrological cycle in regions with significant winter snowfall.

480



485

**Figure 7. Seasonal distribution of key hydroclimatic variables for the reference period (1981–2010), future period (2070–2099), and their average absolute changes across the Matane catchment using both the conventional and asynchronous methods. The figure presents the monthly averages of streamflow, interflow, surface runoff, actual evapotranspiration (ETa), groundwater recharge, and snow water equivalent (SWE). The left column shows the reference period, the middle column displays the future period, and the right column illustrates the absolute changes between the two periods. The shaded areas represent the variability across the climate models.**

Figure 8 presents a comparison of SWE for the reference period (1981–2010) across various climate models in the Matane Catchment. Each panel corresponds to a different climate model, with the shaded areas illustrating the range of annual variability. Similar figures for other catchments are provided in Appendix C (Fig. C1 to Fig. C9).

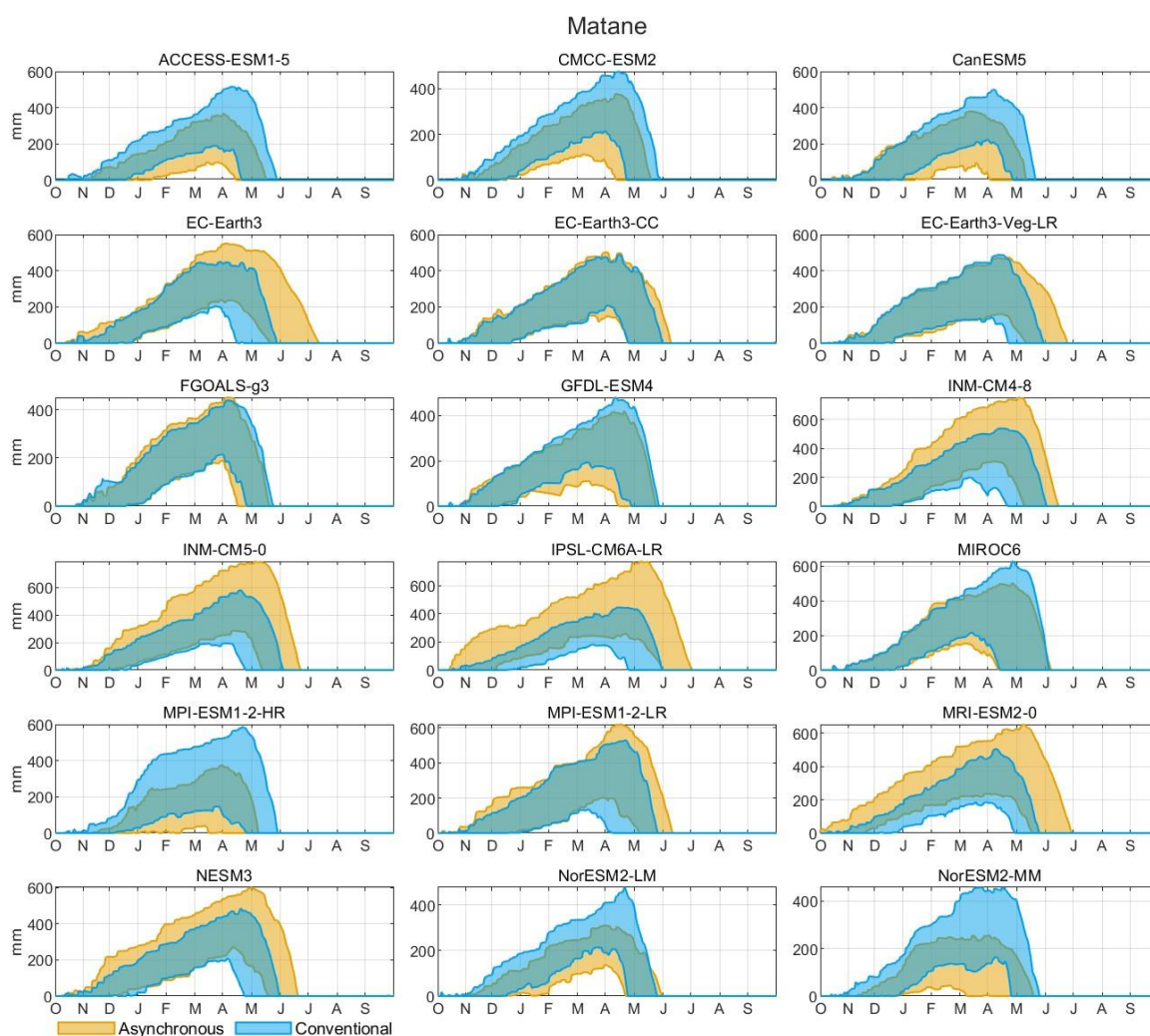
The figure clearly demonstrates the significant variability in SWE results produced by the asynchronous method compared to the conventional method. This disparity underscores the asynchronous method's challenges in accurately simulating snow patterns. For instance, the asynchronous method exhibits a broad range of SWE values, with the NorESM2-MM model showing only 200 mm of snow cover, while the IPSL-CM6A-LR model projects up to 700 mm for the same period. Additionally, the duration of snow accumulation varies widely within the asynchronous method. NorESM2-MM, for example, depicts snow presence from November to May, whereas EC-Earth3 suggests snow from October extending into July. These inconsistencies indicate a potential weakness in the asynchronous method's ability to capture snow dynamics.

495



In contrast, the conventional method consistently produces more stable and realistic results across different climate models, accurately reflecting the expected behaviour of snow accumulation and melt processes.

500 The poor representation of snow processes for asynchronous method is not limited to the Matane catchment. Other catchments, such as Valin and Godbout, exhibit similar anomalies, with snow present from November to September in some cases. Particularly striking is one climate model simulation in the Godbout catchment, where the asynchronous method predicts snow cover persisting throughout 11 months of the year. In the Bras du Nord catchment, the asynchronous method predicts roughly half the amount of snow compared to the conventional method, further highlighting again inadequate  
505 representation of snow accumulation and melt dynamics.



510 **Figure 8. Snow water equivalent (SWE) comparison for the reference period (1981–2010) across various climate models for the Matane Catchment. This figure presents the SWE simulation results from multiple climate models using both the conventional (blue) and asynchronous (yellow) methods. Each panel represents a different climate model, illustrating the seasonal SWE**



accumulation and melt cycle. The shaded areas depict the range of annual variability, highlighting the spread of model outputs and the differences in snow dynamics as captured by each method.

Figure 9 illustrates the spatial distribution of annual groundwater recharge rates in the Matane catchment for both the reference (1981–2010) and future (2070–2099) periods, comparing the results from the conventional and asynchronous methods. Both methods exhibit similar spatial patterns, with higher elevations showing reduced recharge rates and lower elevations demonstrating higher recharge rates. An elevation map of the Matane catchment is provided in the Appendix D (Fig. D1). The asynchronous method, however, predicts a generally higher magnitude of recharge across the catchment.

When examining the absolute difference between the future and reference periods, both methods project a similar spatial pattern of changes in groundwater recharge, with a noticeable decrease in recharge at lower elevations. However, the asynchronous method projects smaller increases in recharge in certain higher elevation areas, while the conventional method predicts a much more pronounced reduction—3 to 4 times greater—at lower elevations.

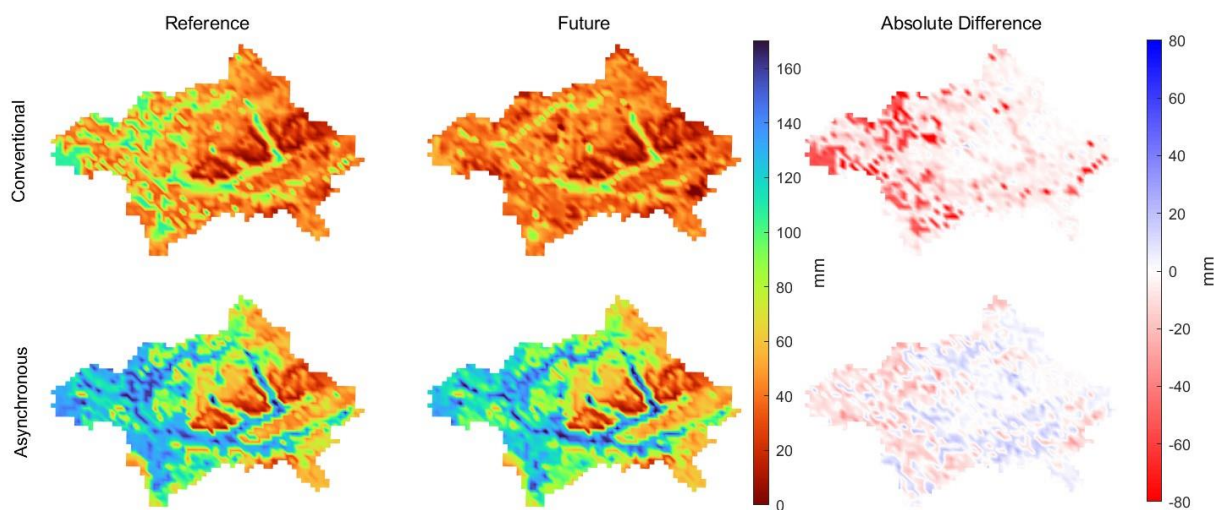


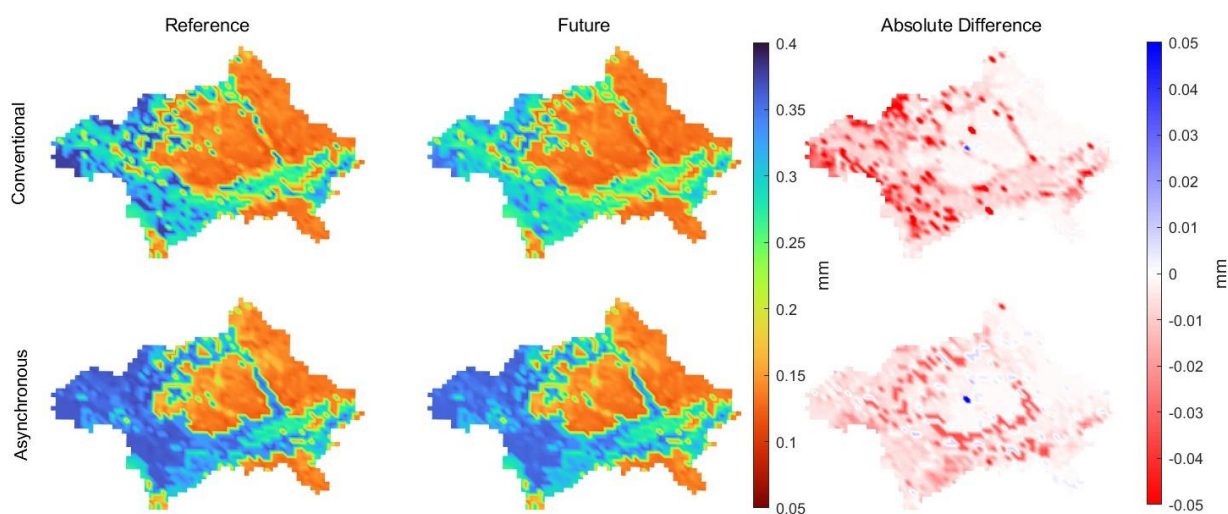
Figure 9. Spatial distribution of annual groundwater recharge in the Matane catchment for the reference period (1981–2010) and future period (2070–2099) using both the conventional and asynchronous methods. The left column shows groundwater recharge (mm) for the reference period, the middle column for the future period, and the right column illustrates the absolute difference between the two periods. The top row represents the conventional method, and the bottom row represents the asynchronous method. The color scale indicates groundwater recharge rates, with warmer colors representing lower recharge and cooler colors indicating higher recharge rates. The absolute difference maps highlight areas of significant change between the two periods, illustrating the spatial variability in projected groundwater recharge changes within the catchment.

Figure 10 illustrates the spatial distribution of soil moisture across the Matane catchment for both the reference period (1981–2010) and the future period (2070–2099), comparing results from the conventional and asynchronous methods. Both methods demonstrate that soil moisture distribution is heavily influenced by soil type, as indicated by the consistent spatial patterns observed (detailed soil type information is provided in the Appendix D, Fig. D1). The soil moisture maps show that areas with finer soils, such as loam, tend to have higher moisture retention, while coarser soils, such as sandy loams, exhibit lower moisture levels.



The asynchronous method tends to generate slightly higher soil moisture values compared to the conventional method, particularly in areas with inherently higher moisture retention capacity. The asynchronous method also displays greater variability in soil moisture patterns.

In terms of absolute changes between the reference and future periods, the conventional method projects a general decrease in soil moisture, predominantly in regions with initially higher moisture values. The asynchronous method, while also projecting a decrease in soil moisture around high moisture areas, shows a more complex pattern with small regions exhibiting increases in soil moisture. Finally, it is noteworthy that the patterns of groundwater and soil moisture during the reference and future periods are spatially consistent and exhibit similar trends.



545 **Figure 10. Spatial distribution of soil moisture in the Matane catchment for the reference period (1981–2010) and future period (2070–2099) using both the conventional and asynchronous methods. The left column shows soil moisture for the reference period, the middle column for the future period, and the right column illustrates the absolute difference between the two periods. The top row represents the conventional method, and the bottom row represents the asynchronous method. The color scale indicates soil moisture levels, with warmer colors representing lower moisture content and cooler colors indicating higher moisture content. The absolute difference maps highlight areas of significant change between the two periods, illustrating the spatial variability in projected soil moisture changes within the catchment.**

#### 4 Discussion

The primary goal of this study was to evaluate the ability of the asynchronous method in reproducing key hydroclimatic processes within a catchment and to compare its performance according to the conventional method. Through detailed analyses across multiple catchments, including a focused case study on the Matane catchment, this study aimed to determine whether the asynchronous method could offer a robust alternative to the conventional method, particularly in the context of climate change impact studies.





#### 4.1 Hydroclimatic variables representation

560 One benefit of the asynchronous method is its ability to better represent extreme higher values (Q95 and Q90) compared to conventional approach. By aligning the flow distribution with observed data, the asynchronous method effectively reproduces the magnitude of these high flow events, which is critical for managing flood risks under future climate conditions.

565 However, despite its strengths in representing streamflow distributions, this study's findings align with other research indicating that the asynchronous method struggles to accurately capture the timing of observed streamflow, particularly during spring high-flow events (Ricard et al., 2023). This issue contrasts with earlier findings by Ricard *et al.* (2020), who reported that the asynchronous modeling approach provided a superior representation of the hydrologic regime compared to the conventional method.

570 The asynchronous method performs comparably to the conventional method when it comes to representing the spatial distribution of hydroclimatic variables such as soil moisture and groundwater recharge. This similarity is likely due to the strong correlation between these hydroclimatic variables and the physical properties of the catchment, such as elevation and soil type (Talbot et al., 2024b). The consistent representation of these variables across both methods suggests that the fundamental physical processes driving these patterns are well-captured, irrespective of the methodological differences in how streamflow is simulated.

575 The asynchronous method shows consistency with the conventional method in predicting the overall trends for several variables, such as increases in precipitation and ETa, as well as decreases in SWE and snowfall. These findings align with broader climate change projections for the region, which anticipate warmer temperatures leading to reduced snow accumulation and altered precipitation patterns (Aygün et al., 2022; Nolin et al., 2023; Valencia Giraldo et al., 2023; Talbot et al., 2024b). However, while the overall trends may appear consistent, the underlying processes and the accuracy of the projections differ significantly between the two methods.

580 Despite these consistencies, a significant issue with the asynchronous method is its high sensitivity to variability in climate models. This problem comes from the biases inherent in climate models, which often lead to the simulation of hydrological processes occurring either too early or too late (Chen et al., 2021; Ricard et al., 2023). The asynchronous method, as currently implemented, adjust the calibration parameters to correct for biases, assuming that these biases remain constant over time. Consequently, if a climate model has a significant or nonstationary biases, the asynchronous method will 585 perpetuate these biases, leading to inaccuracies in the timing of peak flows and the representation of hydroclimatic variables. Ricard et al. (2023) also emphasizes this vulnerability, noting that the asynchronous method is particularly prone to producing outlying projections due to the uncorrected biases in raw climate model outputs.

One of the most critical issues highlighted in this study is the concept of equifinality, where different models or methods achieve similar outcomes for different reasons (Mei et al., 2023; Yassin et al., 2017). In the case of the asynchronous



590 method, it appears to replicate certain aspects of the conventional method's projections, but it does so through potentially  
flawed mechanisms.

The asynchronous method struggles to synchronize streamflow with the actual timing of hydrological events, particularly  
snowmelt. This lack of synchronization leads to a cascade of flawed mechanisms throughout the model. For instance, when  
snowmelt occurs too early or too late, the timing and magnitude of surface runoff are inaccurately represented, which can  
595 lead to unrealistic increases in surface runoff during inappropriate seasons. This misalignment also affects evapotranspiration  
and groundwater recharge, causing large, unrealistic variations, further skewing the model's output. Because the streamflow  
is not properly synchronized with the seasonal dynamics, the asynchronous method ultimately produces streamflow  
simulations that may match the overall distribution of the observations but do so for the wrong reasons.

Equifinality becomes particularly problematic in this context because the asynchronous method may achieve similar  
600 projected changes in hydroclimatic variables as the conventional method, but for reasons that are not hydrologically sound.  
This brings into question the reliability of its projections, especially when the method demonstrates high variability among  
different climate models. Such variability, coupled with the method's inability to accurately replicate key hydrological  
processes, suggests that the asynchronous method, as implemented in this study, may not provide a robust framework for  
analyzing climate change impacts on hydroclimatic variables.

605 In contrast, the conventional method excels at addressing the timing of hydrological events due to its optimization process,  
which incorporates the synchronization between observed and simulated flows. This synchronization allows the model to  
more accurately capture the timing of hydrological processes, such as snowmelt and peak flows. Given the importance of  
this synchronicity, it would be beneficial for the asynchronous method to integrate a similar measure of event timing. This  
adjustment could pave the way for a semi-asynchronous approach that balances the strengths of both methods, offering better  
610 overall performance in hydrological simulations.

#### 4.2 Advantages and limitations

Both the conventional and asynchronous methods present distinct advantages and limitations. One of the most notable  
distinctions between the two methods lies in how they handle extremes. The Multivariate Bias Correction (MBCn) approach,  
typically used in the conventional method, tends to dampen the extremes, smoothing out the peaks. In contrast, the  
615 asynchronous method, which calibrates directly on the distribution of streamflow without bias correction, preserves (or  
attempts to preserve) these extremes (Ricard et al., 2023). Maintaining extreme values may provide a more realistic  
representation of potential high-impact events.

Another critical consideration is the computational demand of the asynchronous method. Due to its reliance calibration on  
every climate model, the asynchronous method requires significantly more computational time in the calibration process.  
620 This increased computational cost must be weighed against the benefits of using the asynchronous method, particularly when  
the conventional method might achieve similar results with less computational effort and more established reliability.



The performance of the asynchronous method in snow-dominated catchments has proven to be problematic in this study. The method's inability to accurately capture snowmelt processes, as evidenced by the unrealistic snow retention and melt timing, casts doubt on its utility in regions where snow dynamics play a critical role in the hydrological cycle. Additionally, the high variability observed between climate models when using the asynchronous method suggests that the approach may be overly sensitive to the inherent uncertainties present in raw climate data. This variability complicates the interpretation of results and diminishes confidence in the method's projections, particularly in scenarios where precise predictions are required for decision-making.

The key takeaway from this study is that while the asynchronous method allowed preserving the distribution of streamflow and maintaining extremes, it does so at the cost of increased variability and potential inaccuracies in simulating critical hydrological processes, particularly those related to snow. Therefore, the asynchronous method, as implemented in this study, should be used with caution, especially in snow-dominated catchments where accurate representation of snowmelt is crucial. However, the asynchronous method could be useful in scenarios where the distribution of extremes is of particular interest, such as in regions where the temporal distribution of streamflow is less critical than the overall volume

The conventional method, which is optimized to account for event-specific dynamics, remains the more reliable option for most applications, particularly when the goal is to simulate the timing and magnitude of streamflow events with a higher degree of accuracy.

Ultimately, these findings aim to inform decision-making in critical sectors such as agriculture, water resource management, urban planning, and environmental conservation. For example, soil moisture data is essential in agriculture for optimizing irrigation and improving crop yields, as well as in environmental management for maintaining wetlands and forest ecosystems. Groundwater recharge data supports sustainable management of aquifers, which is crucial for drinking water supplies, agriculture, and industrial use, while also guiding urban planning to avoid flooding or subsidence. Surface runoff modeling is vital for flood prevention and urban infrastructure design, ensuring stormwater systems can handle heavy rainfall. Lastly, streamflow data is key to water resource management, enabling efficient allocation for agriculture and industry, flood forecasting, and optimizing hydroelectric power generation. By providing detailed projections of these key hydroclimatic variables, this study supports adaptive management strategies across a wide range of sectors impacted by climate change.

### 4.3 Future directions

Looking forward, one of the most promising avenues for improving the asynchronous method is the integration of synchronicity, leading to the development of a semi-asynchronous approach. This hybrid method would combine the strengths of both the conventional and asynchronous methods, offering a more balanced solution that mitigates the weaknesses observed in each. By incorporating synchronicity into the calibration process, the semi-asynchronous method would better align the timing of hydrological events, such as snowmelt, with observed data, improving its ability to capture critical seasonal dynamics.



655 For instance, modifying the objective function to calibrate based on seasonal or monthly data could enhance the model's ability to simulate hydrological processes. This integration of event timing into the calibration process is crucial for addressing the timing discrepancies that currently limit the asynchronous method's performance.

In parallel, ongoing advancements in climate modeling provide an opportunity to further refine the semi-asynchronous approach. As climate models become more accurate, with fewer biases and enhanced temporal precision, the challenges of  
660 synchronization in the current asynchronous method could be significantly alleviated. These improvements would enable the semi-asynchronous method to offer more robust and reliable simulations of hydrological processes under future climate scenarios, positioning it as a more versatile tool for climate impact assessments.

## 5 Conclusion

This study aimed to evaluate the performance of the asynchronous method in comparison to the conventional method for  
665 simulating key hydroclimatic variables within catchments, with a focus on the implications for climate change impact studies. Through a detailed analysis of multiple catchments, including a focused case study on the Matane catchment, the study has revealed several important insights into the strengths and limitations of both methods.

The findings indicate that while the asynchronous method shows promise in accurately preserving extreme values, it struggles significantly with the timing of hydrological events, particularly those related to snowmelt. This timing issue is  
670 critical in snow-dominated catchments, where accurate snowmelt representation is crucial for reliable hydrological modeling. The asynchronous method's vulnerability to equifinality, nonstationarity and biases in climate models further complicates its application, often leading to increased variability and potential inaccuracies in key hydrological processes which may not be hydrologically sound.

In contrast, the conventional method, with its bias correction step, provides more reliable simulations of event-specific  
675 dynamics, particularly in capturing the timing and magnitude of streamflow events, but at cost of underestimating extreme hydrological events. This reliability makes it a more suitable choice for most hydrological applications, especially in regions where precise timing of hydrological events is essential.

From a practical standpoint, while the asynchronous method offers the advantage of preserving extremes, it comes at the cost of increased computational demand and variability in projections, which may limit its utility in certain contexts. The  
680 conventional method, on the other hand, remains a robust and reliable tool for simulating hydrological processes under future climate scenarios, particularly when accuracy in timing is a critical factor.

Looking ahead, there are significant opportunities to refine the asynchronous method, particularly by integrating synchronicity into the calibration process to better capture seasonal dynamics. This enhancement could lead to the development of a semi-asynchronous approach that combines the strengths of both the asynchronous and conventional  
685 methods, addressing the current challenges related to event timing while preserving the ability to model extremes. Such a



hybrid method would offer a more balanced solution, improving accuracy in snowmelt representation and other critical hydrological processes.

690 Until these refinements are realized, the asynchronous method should be applied with caution, especially in regions where precise seasonal dynamics, such as snowmelt, are critical. Future research should focus on advancing the semi-asynchronous method, ultimately aiming to create a more versatile and robust tool for hydrological modeling in the context of climate change.

## Appendix A

**Table A1. Kling-Gupta Efficiency (KGE) values for the conventional method during the calibration and validation periods across ten catchments. The mean KGE values for calibration and validation are also provided.**

Conventional Method	Area (km <sup>2</sup> )	KGE	
		Calibration	Validation
Bonaventure	1910	0.847	0.889
Matane	1650	0.906	0.906
Ouelle	795	0.894	0.834
Bécancour	919	0.850	0.807
Nicolet Sud-Ouest	549	0.817	0.786
Au Saumon	738	0.831	0.778
Bras du Nord	642	0.873	0.872
Du Loup	774	0.838	0.804
Valin	746	0.902	0.885
Godbout	1570	0.869	0.863
	Mean	0.863	0.842

695

700

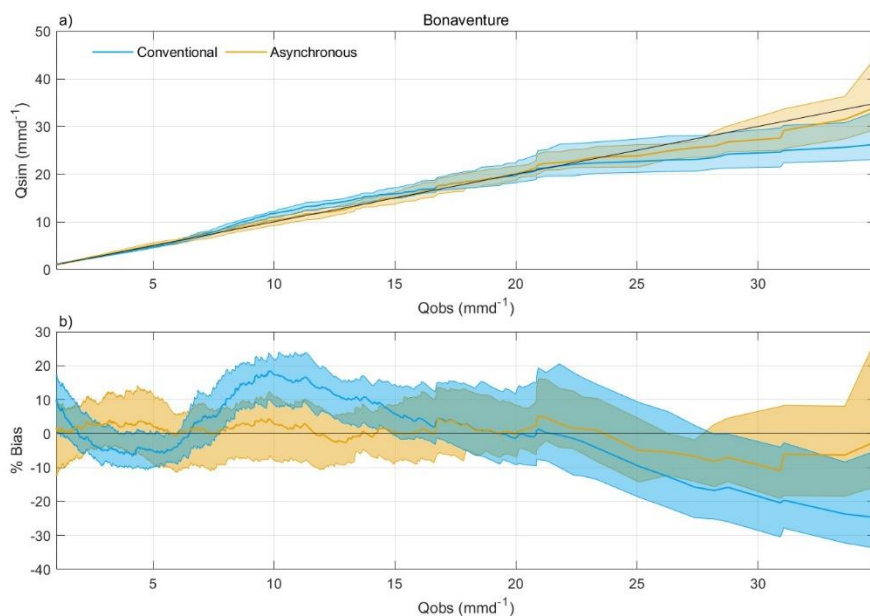


**Table A2. Root Mean Square Error (RMSE) values for the asynchronous method during the calibration and validation periods across ten catchments. The mean RMSE values for calibration and validation are also provided.**

Asynchronous Method		RMSE			
		Calibration		Validation	
Name	Area (km <sup>2</sup> )	Mean	Std	Mean	Std
Bonaventure	1910	0.108	0.031	0.154	0.047
Matane	1650	0.124	0.021	0.180	0.034
Ouelle	795	0.125	0.027	0.167	0.043
Bécancour	919	0.095	0.019	0.158	0.048
Nicolet Sud-Ouest	549	0.125	0.034	0.200	0.097
Au Saumon	738	0.156	0.054	0.209	0.053
Bras du Nord	642	0.175	0.044	0.243	0.063
Du Loup	774	0.085	0.019	0.165	0.091
Valin	746	0.109	0.036	0.162	0.055
Godbout	1570	0.110	0.032	0.157	0.037
	Mean	0.121	0.031	0.179	0.057



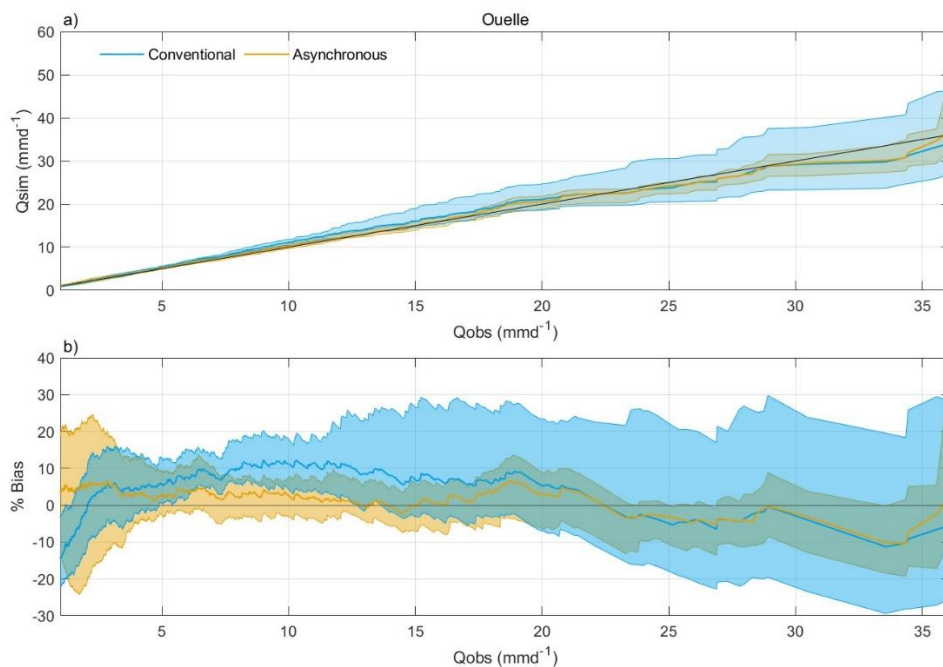
## Appendix B



705

710

**Figure B1.** Performance comparison between the conventional and asynchronous methods for the Bonaventure catchment during the reference period (1981–2010). Panel (a) displays the relationship between simulated daily streamflow ( $Q_{sim}$ ) and observed daily streamflow ( $Q_{obs}$ ) for the conventional (blue) and asynchronous (yellow) methods. The x-axis represents the observed daily streamflow, while the y-axis represents the simulated streamflow. Panel (b) shows the percentage bias between observed and simulated streamflows for both methods, with the x-axis representing the observed daily streamflow and the y-axis displaying the percentage bias relative to the observed values. The shaded regions in both panels illustrate the variability among climate models around the mean bias for each method, emphasizing the differences in how well each method simulates streamflow across the observed streamflow range.



715 **Figure B2.** Same as Fig. B1, but for Ouelle catchment.

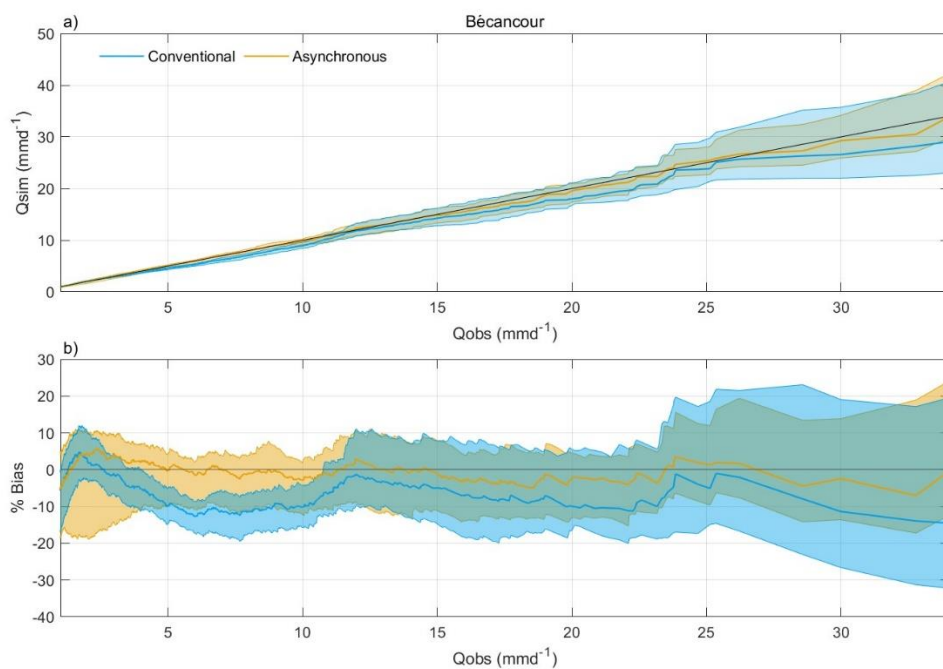


**Figure B3.** Same as Fig. B1, but for Bécancour catchment.



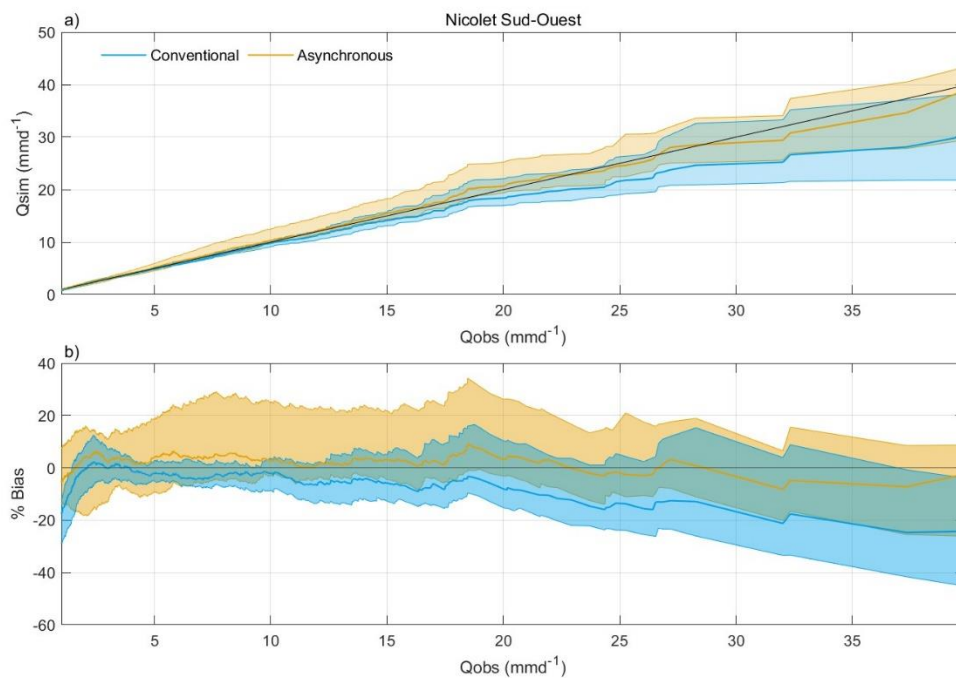


Figure B4. Same as Fig. B1, but for Nicolet Sud-Ouest catchment.

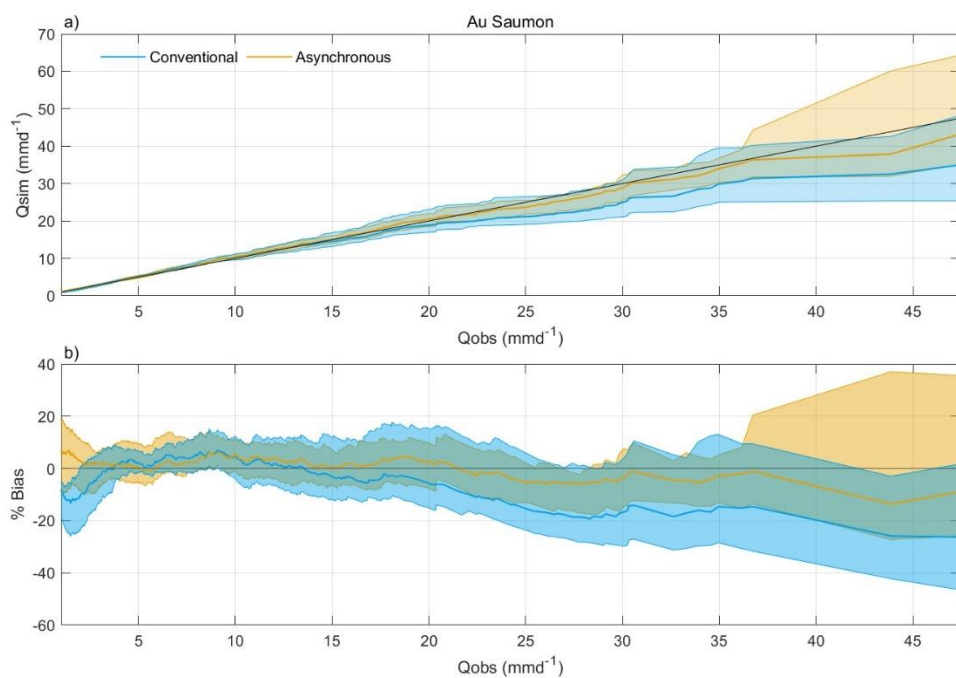


Figure B5. Same as Fig. B1, but for Au Saumon catchment.

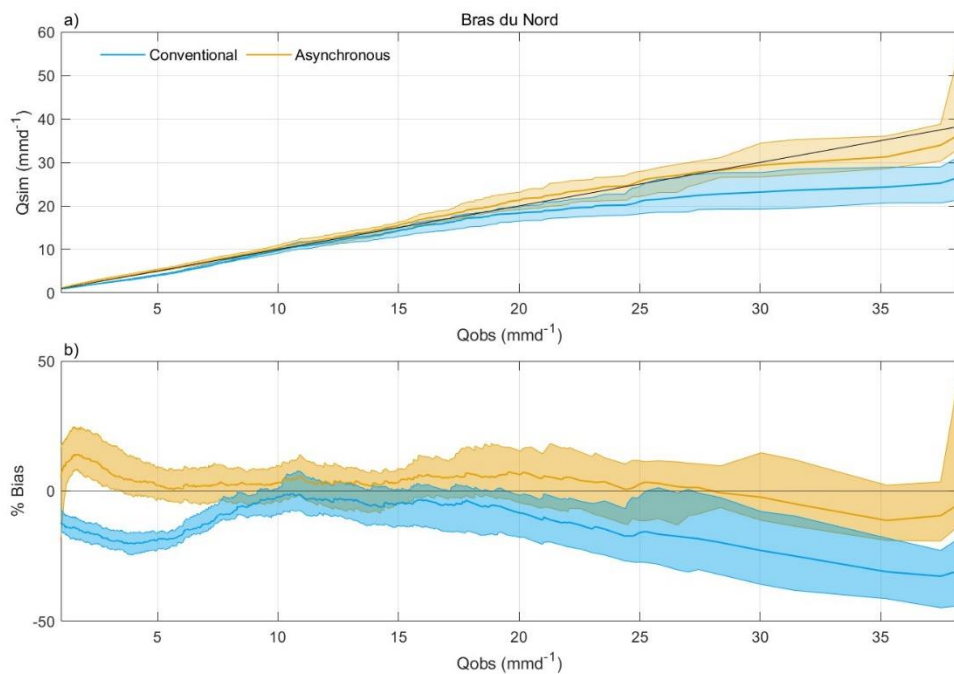
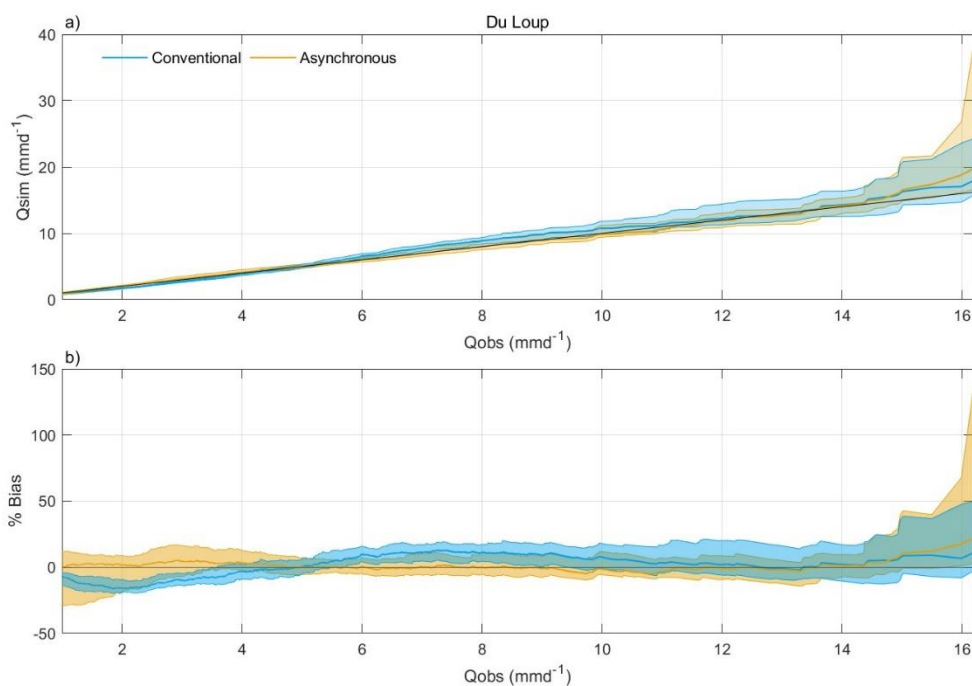
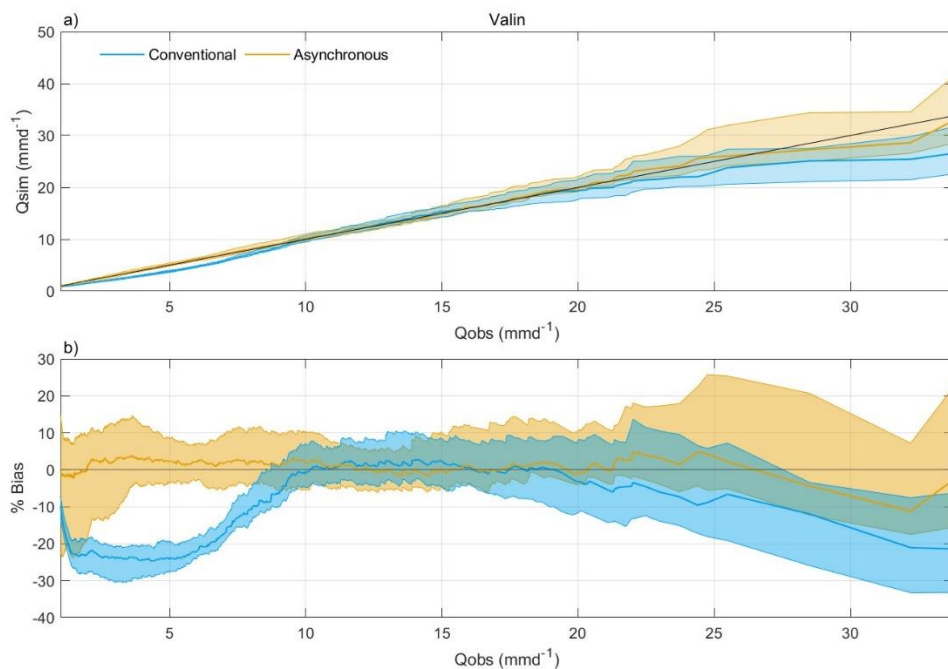


Figure B6. Same as Fig. B1, but for Bras du Nord catchment.



725 Figure B7. Same as Fig. B1, but for Du Loup catchment.



**Figure B8.** Same as Fig. B1, but for Valin catchment.

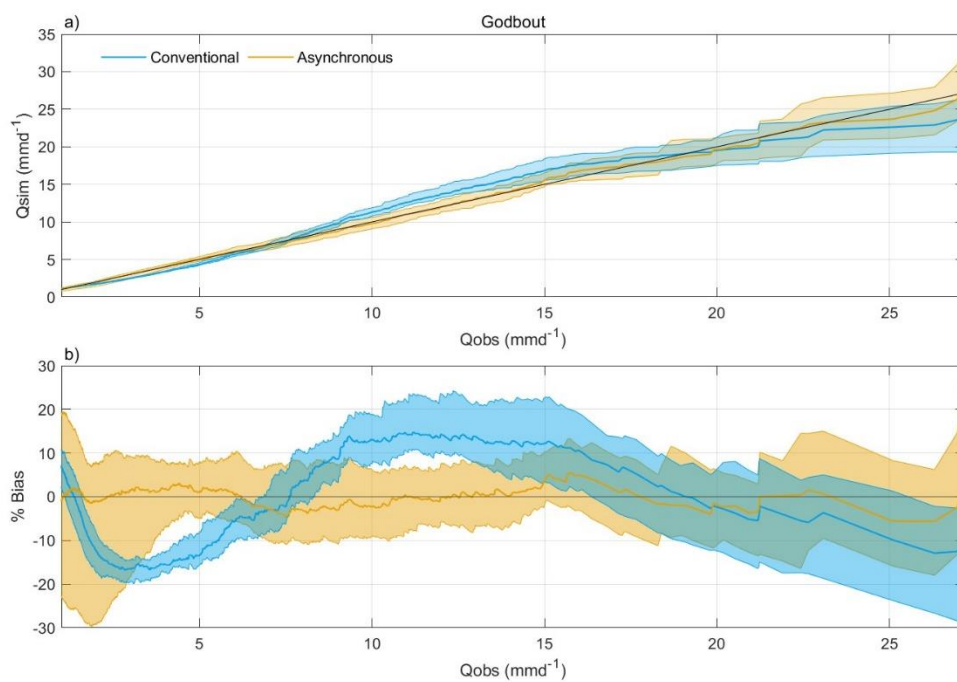


**Figure B9.** Same as Fig. B1, but for Godbout catchment.



## Appendix C

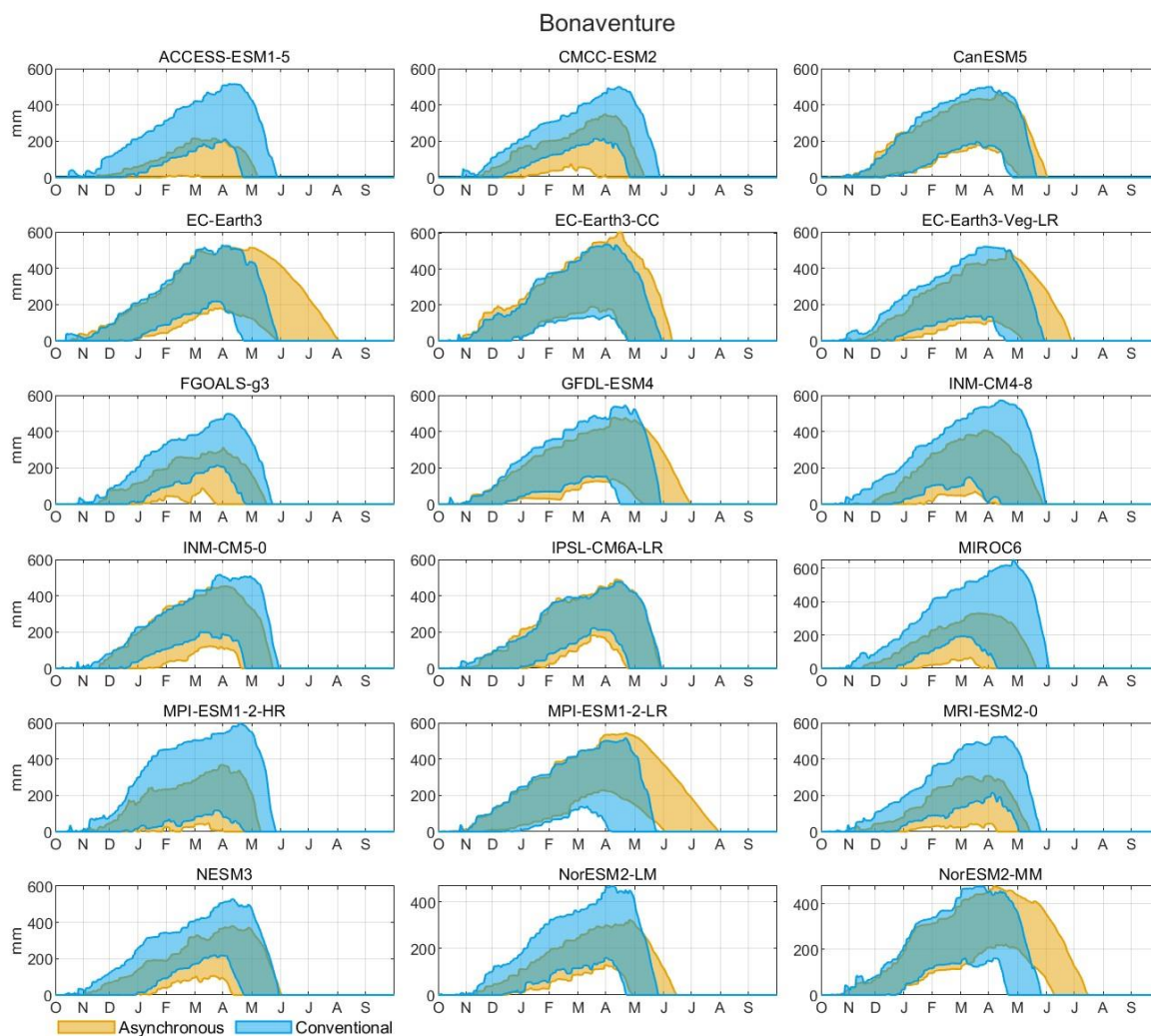


**Figure C1.** Snow water equivalent (SWE) comparison for the reference period (1981–2010) across various climate models for the Bonaventure Catchment. This figure presents the SWE simulation results from multiple climate models using both the conventional (blue) and asynchronous (yellow) methods. Each panel represents a different climate model, illustrating the seasonal SWE accumulation and melt cycle. The shaded areas depict the range of annual variability, highlighting the spread of model outputs and the differences in snow dynamics as captured by each method.

735

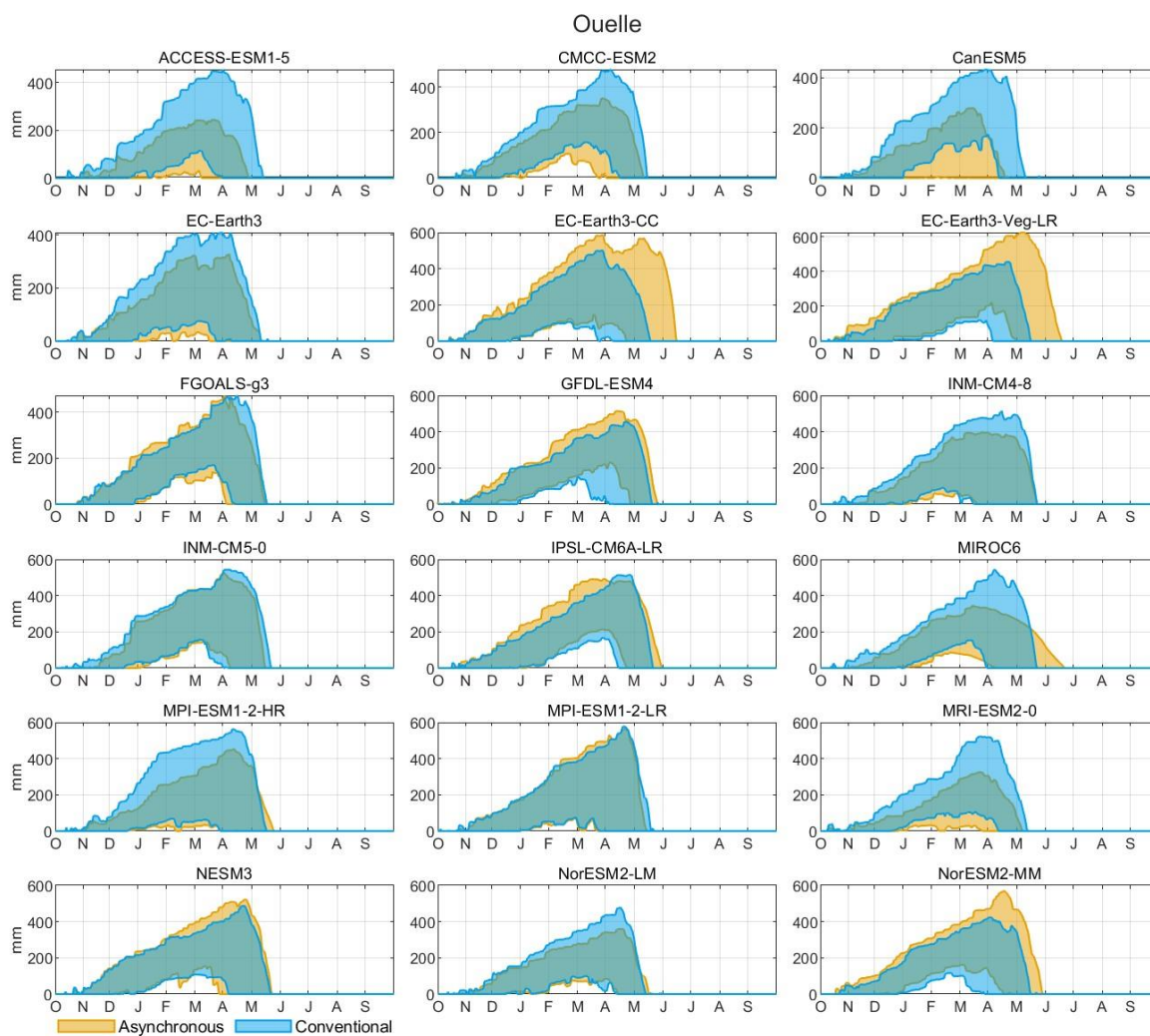
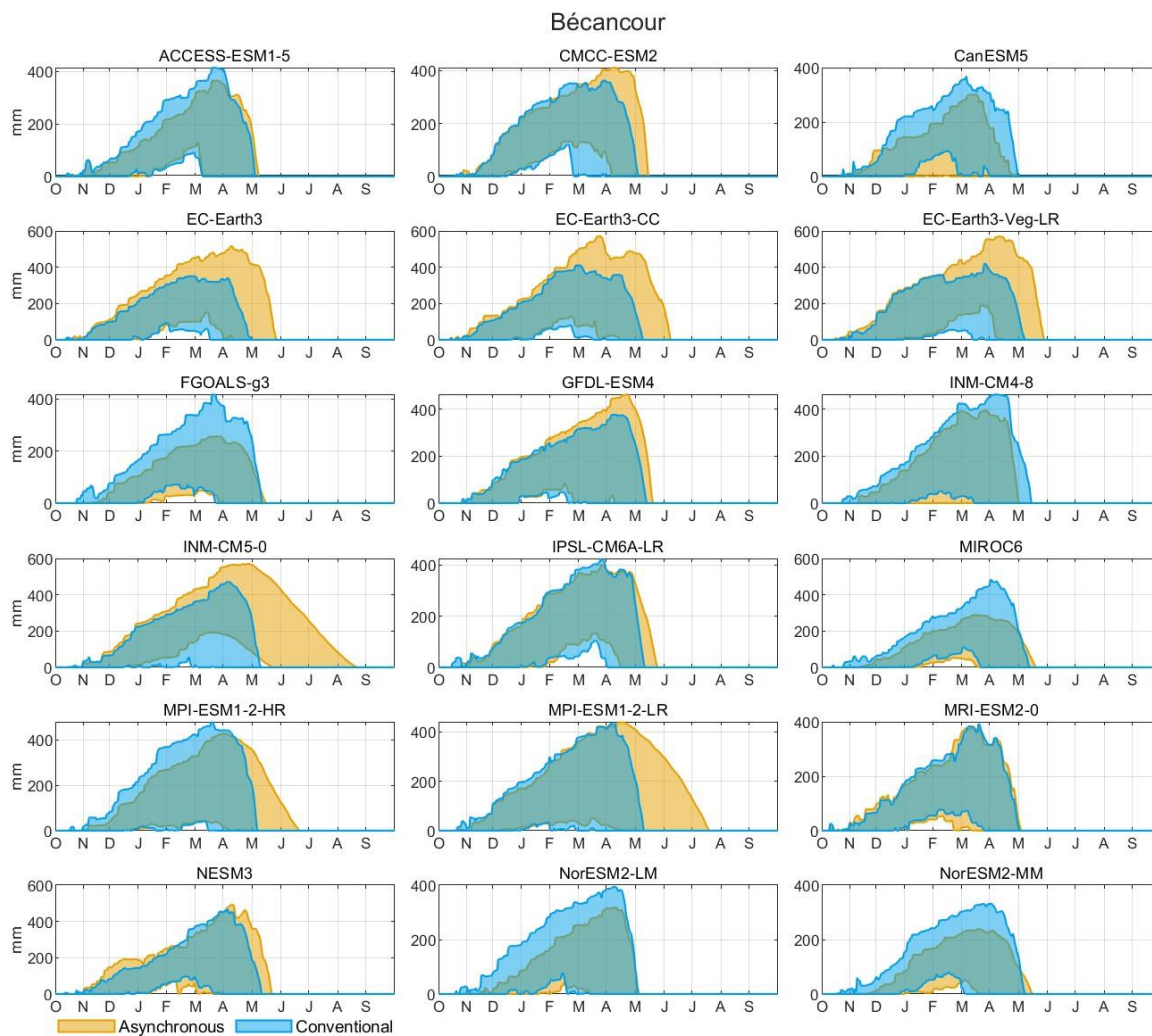


Figure C2. Same as Fig. C1, but for Ouelle catchment.



740

**Figure C3.** Same as Fig. C1, but for Bécancour catchment.

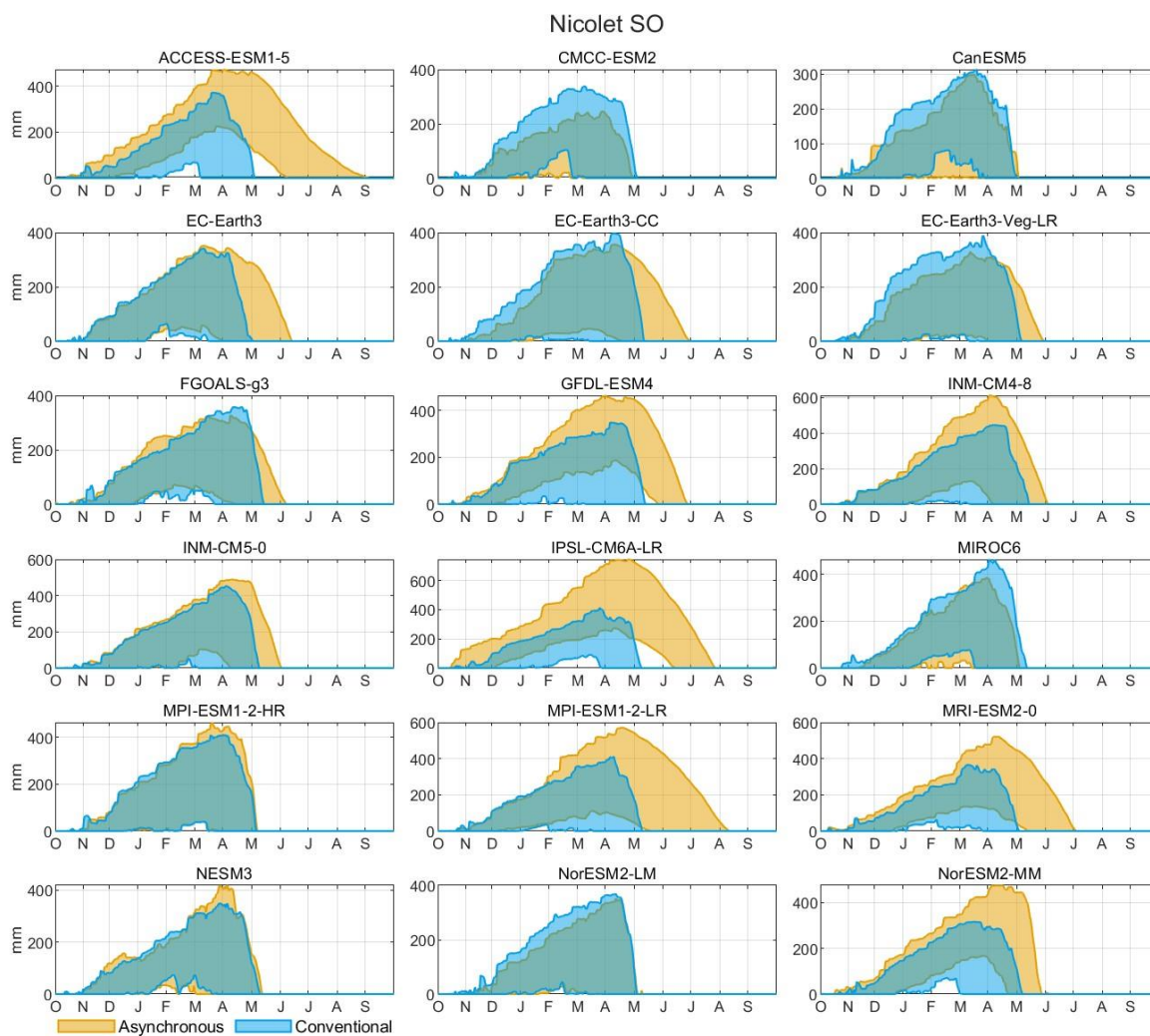
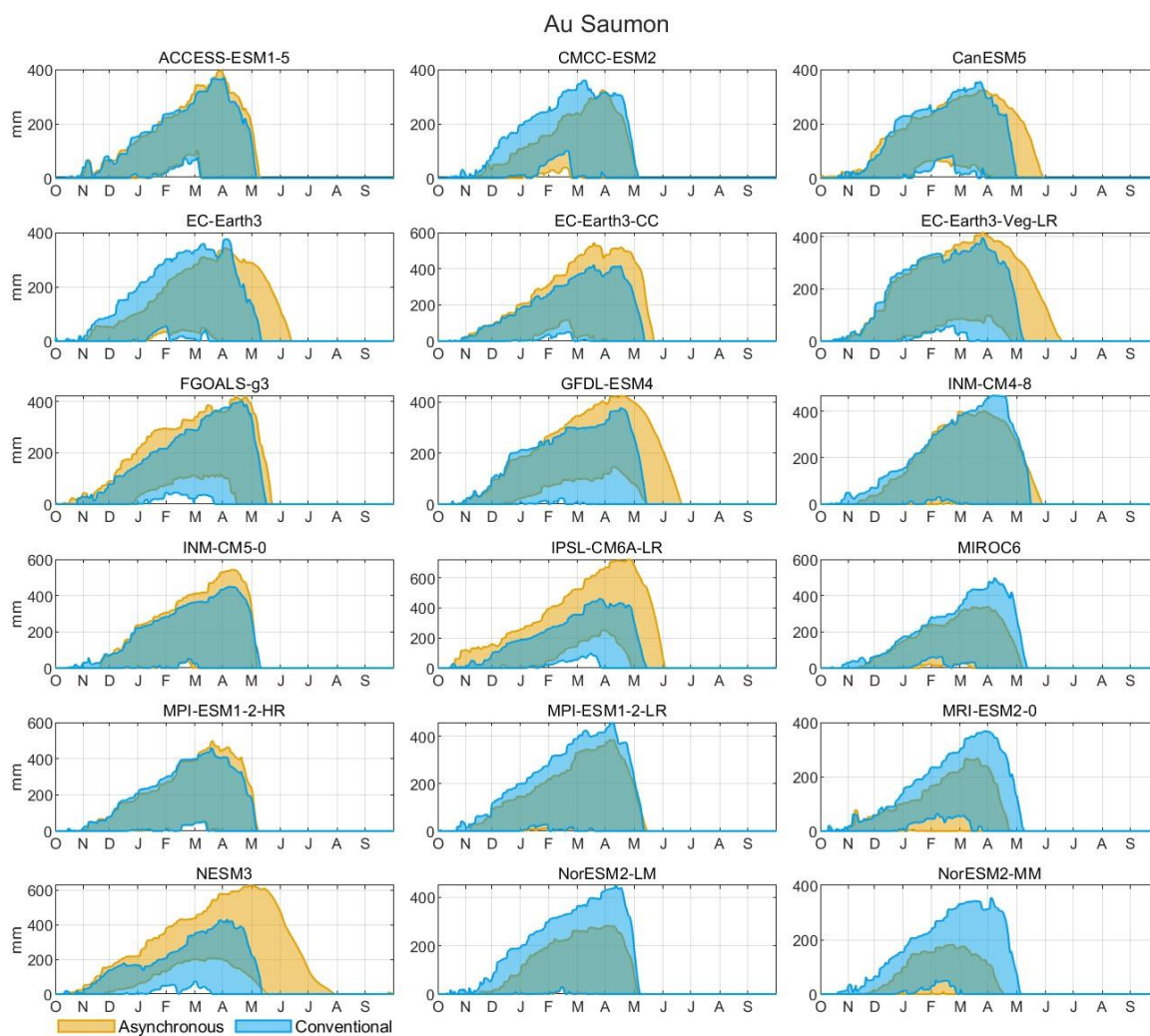
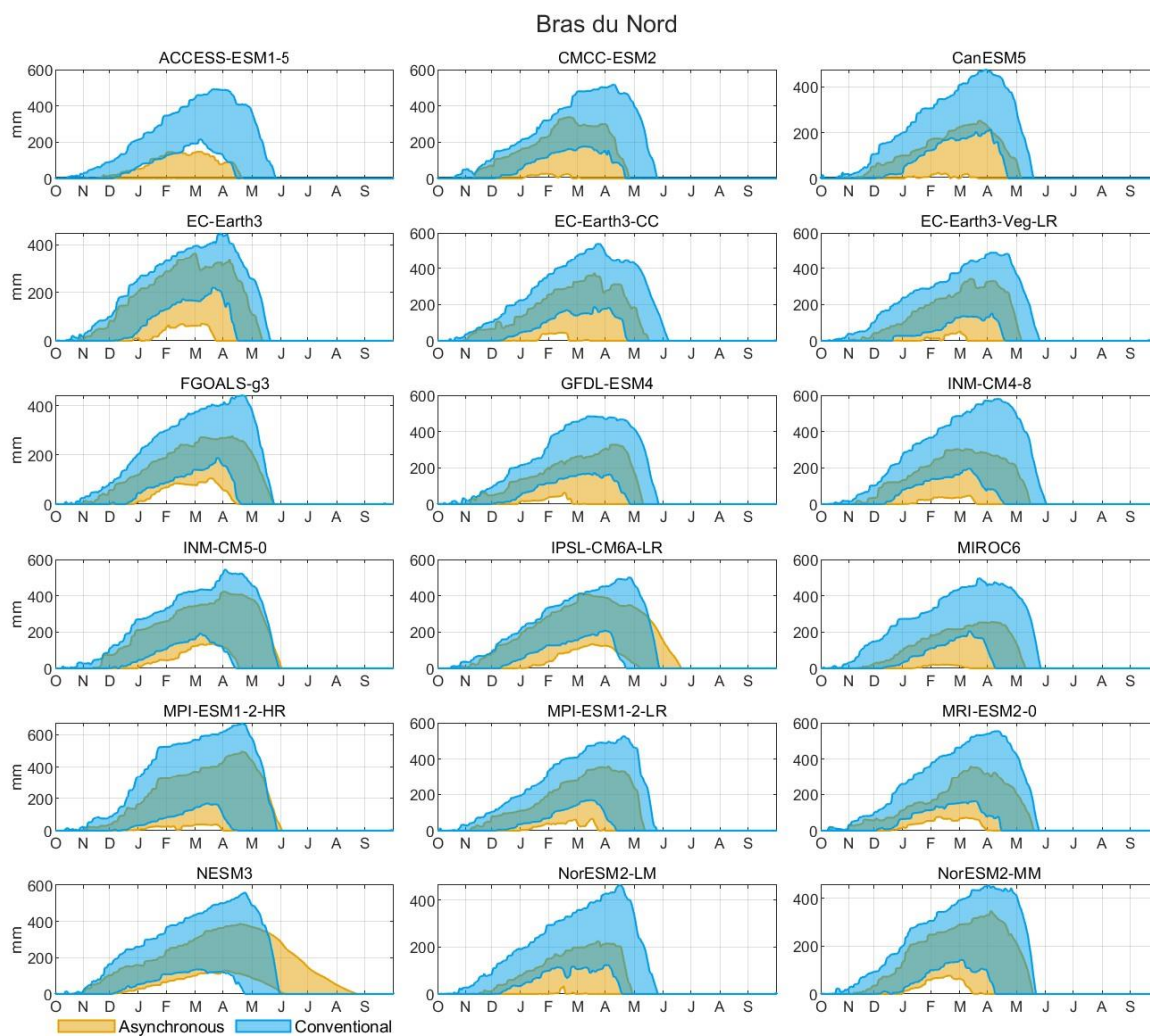


Figure C4. Same as Fig. C1, but for Nicolet Sud-Ouest catchment.



745 Figure C5. Same as Fig. C1, but for Au Saumon catchment.





**Figure C6.** Same as Fig. C1, but for Bras du Nord catchment.

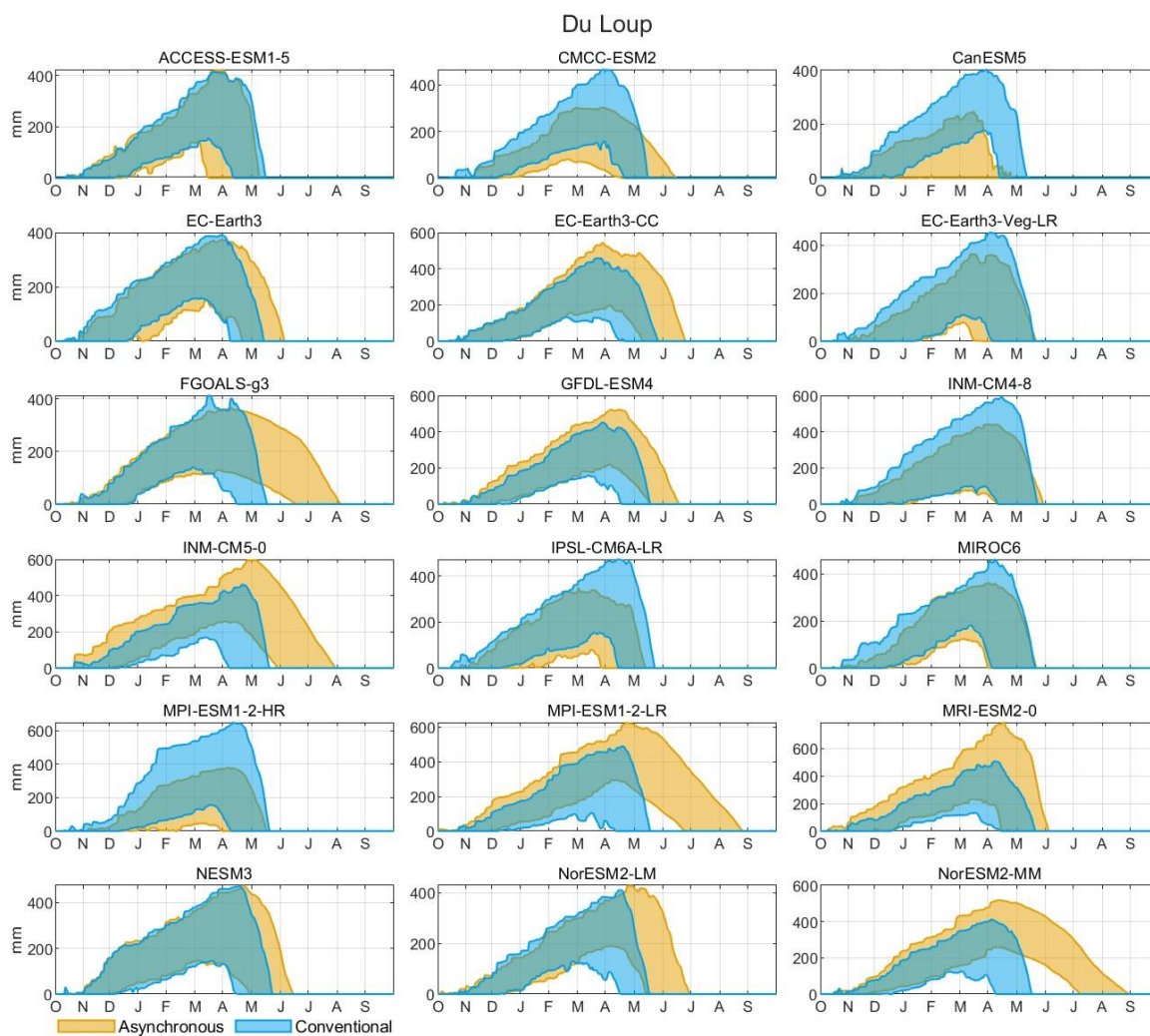
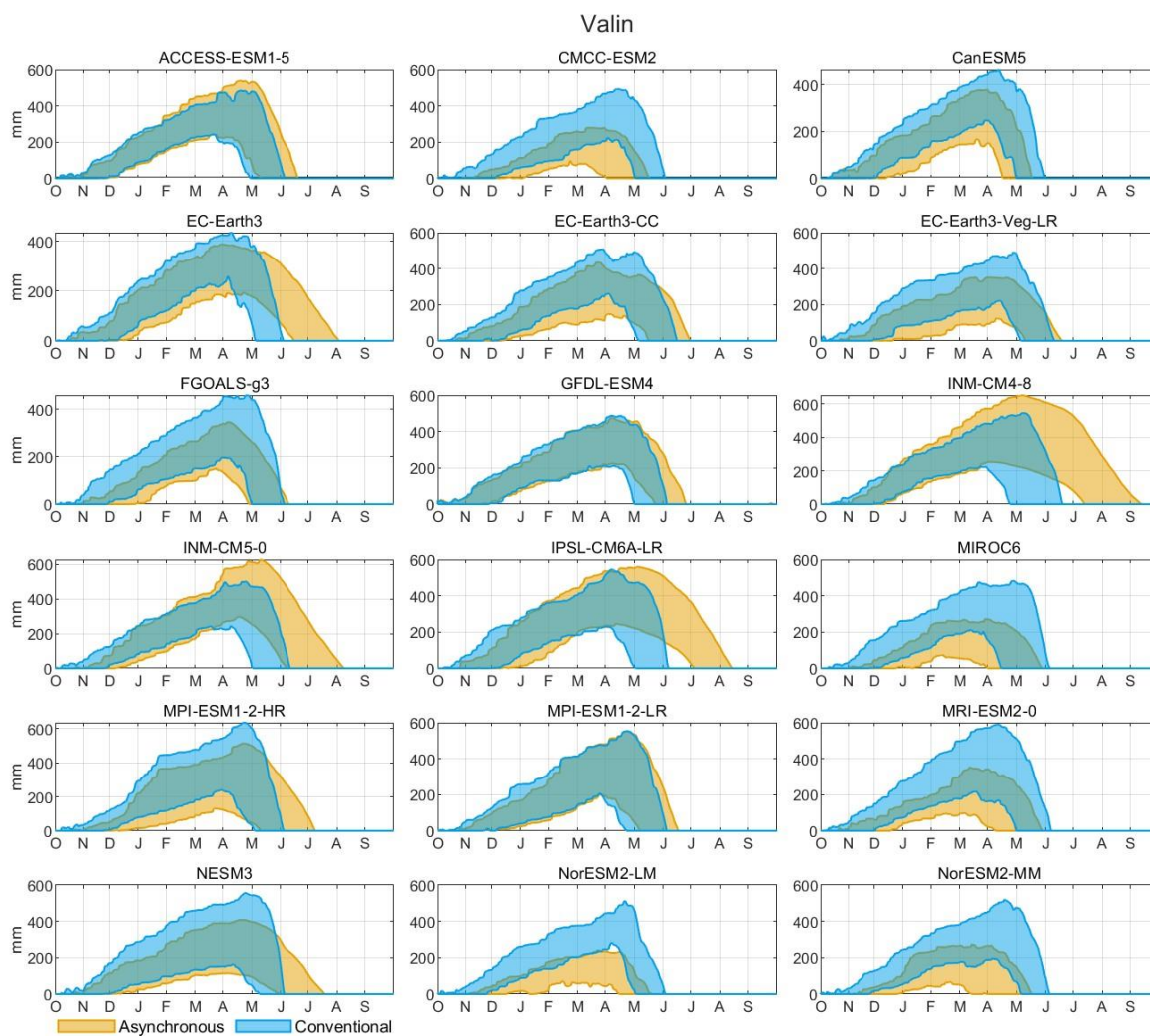


**Figure C7.** Same as Fig. C1, but for Du Loup catchment.



750

Figure C8. Same as Fig. C1, but for Valin catchment.

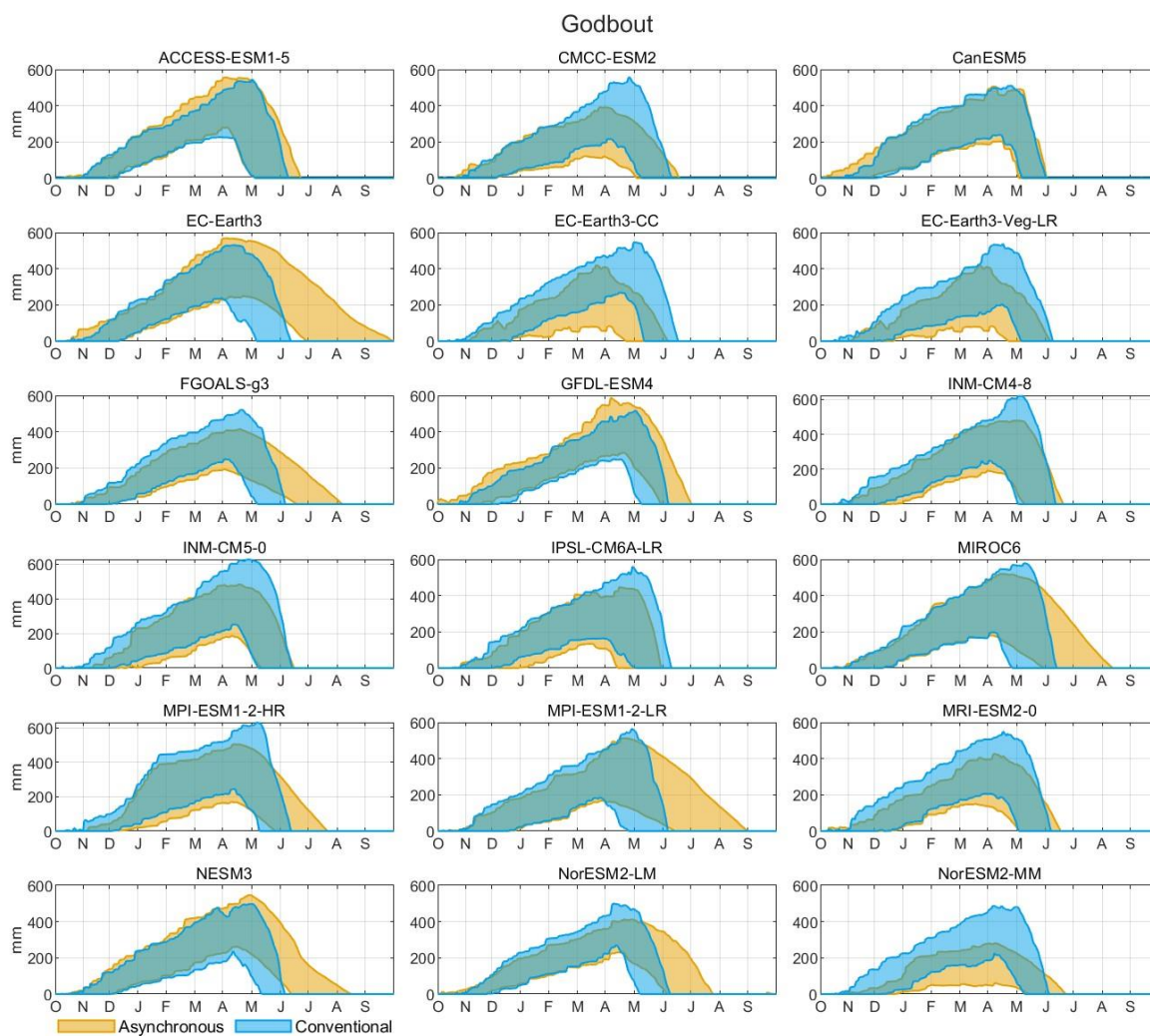
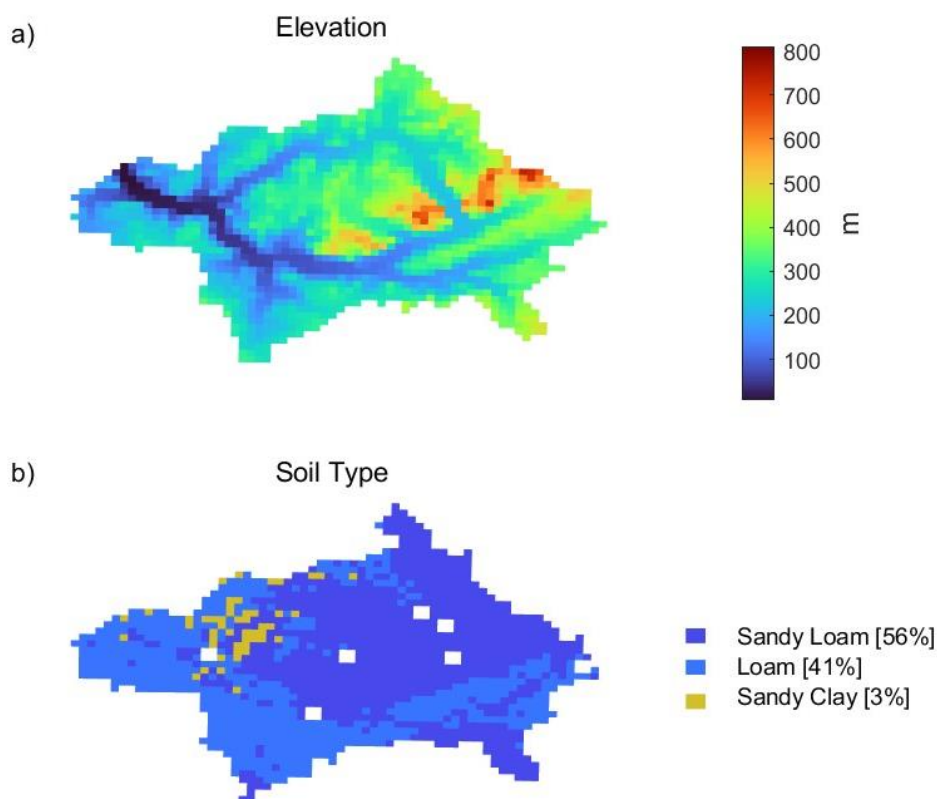


**Figure C9.** Same as Fig. C1, but for Godbout catchment.



## Appendix D



755

**Figure D1.** Topographic and soil type characteristics of the Matane catchment. Panel (a) shows the elevation map, with elevations ranging from 100 to 800 meters above sea level. Higher elevations are indicated in warmer colors (reds and oranges), while lower elevations are shown in cooler colors (blues and greens). Panel (b) displays the distribution of soil types within the catchment, with sandy loam covering 56% of the area (dark blue), loam covering 41% (light blue), and sandy clay occupying 3% (yellow).

## 760 Code and data availability

The calibrated WaSiM model and all simulations for all catchments discussed in this study is publicly accessible at <https://osf.io/n87ey/> (Talbot et al., 2024c).

## Author contribution

765 FT, JDS, SR, and RA contributed to the conceptualization and methodology design of the study. FT performed the formal analysis, investigation, data curation, and conducted the model simulations. JLM contributed to the MBCn post-processing of climate data ensembles. FT was responsible for visualization and led the original draft preparation. JDS and RA provided



supervision and project administration. AP, GD, JDS, RA, SR, JLM and FT contributed to the writing, review, and editing of the manuscript.

### **Competing interests**

770 The authors declare that they have no conflict of interest.

### **Acknowledgements**

This work was funded jointly by the ministère des Ressources naturelles et des Forêts (Quebec, Canada, project number 112332187 conducted at the Direction de la recherche forestière and led by Jean-Daniel Sylvain) and the Forest research service contract number 3322-2022-2187-01 obtained by Richard Arsenault from the Ministère des Ressources naturelles et des Forêts (Quebec, Canada). The authors also acknowledge the use of ChatGPT-4 for assistance in correcting spelling mistakes and improving the flow of text during the manuscript preparation process. The base map in Fig. 1 was created using ArcGIS® software by Esri. ArcGIS® and ArcMap™ are the intellectual property of Esri and are used herein under license. Copyright © Esri. All rights reserved. For more information about Esri® software, please visit [www.esri.com](http://www.esri.com).



## 780 References

- Arsenault, R., Brissette, F., Malo, J.-S., Minville, M., and Leconte, R.: Structural and Non-Structural Climate Change Adaptation Strategies for the Péribonka Water Resource System, *Water Resour Manage*, 27, 2075–2087, <https://doi.org/10.1007/s11269-013-0275-6>, 2013.
- Arsenault, R., Poulin, A., Côté, P., and Brissette, F.: Comparison of Stochastic Optimization Algorithms in Hydrological  
785 Model Calibration, *Journal of Hydrologic Engineering*, 19, 1374–1384, [https://doi.org/10.1061/\(ASCE\)HE.1943-5584.0000938](https://doi.org/10.1061/(ASCE)HE.1943-5584.0000938), 2014.
- Arsenault, R., Brissette, F., Chen, J., Guo, Q., and Dallaire, G.: NAC2H: The North American Climate Change and Hydroclimatology Data Set, *Water Resources Research*, 56, e2020WR027097, <https://doi.org/10.1029/2020WR027097>, 2020.
- 790 Arsenault, R., Huard, D., Martel, J.-L., Troin, M., Mai, J., Brissette, F., Jauvin, C., Vu, L., Craig, J. R., Smith, T. J., Logan, T., Tolson, B. A., Han, M., Gravel, F., and Langlois, S.: The PAVICS-Hydro platform: A virtual laboratory for hydroclimatic modelling and forecasting over North America, *Environmental Modelling & Software*, 168, 105808, <https://doi.org/10.1016/j.envsoft.2023.105808>, 2023.
- Aygiün, O., Kinnard, C., Campeau, S., and Pomeroy, J. W.: Landscape and climate conditions influence the hydrological  
795 sensitivity to climate change in eastern Canada, *Journal of Hydrology*, 615, 128595, <https://doi.org/10.1016/j.jhydrol.2022.128595>, 2022.
- Beck, H. E., Zimmermann, N. E., McVicar, T. R., Vergopolan, N., Berg, A., and Wood, E. F.: Present and future Köppen-Geiger climate classification maps at 1-km resolution, *Sci Data*, 5, 180214, <https://doi.org/10.1038/sdata.2018.214>, 2018.
- Bormann, H. and Elfert, S.: Application of WaSiM-ETH model to Northern German lowland catchments: model  
800 performance in relation to catchment characteristics and sensitivity to land use change, *Adv. Geosci.*, 27, 1–10, <https://doi.org/10.5194/adgeo-27-1-2010>, 2010.
- Calvin, K., Dasgupta, D., Krinner, G., Mukherji, A., Thorne, P. W., Trisos, C., Romero, J., Aldunce, P., Barrett, K., Blanco, G., Cheung, W. W. L., Connors, S., Denton, F., Diongue-Niang, A., Dodman, D., Garschagen, M., Geden, O., Hayward, B., Jones, C., Jotzo, F., Krug, T., Lasco, R., Lee, Y.-Y., Masson-Delmotte, V., Meinshausen, M., Mintenbeck, K., Mokssit, A.,  
805 Otto, F. E. L., Pathak, M., Pirani, A., Poloczanska, E., Pörtner, H.-O., Revi, A., Roberts, D. C., Roy, J., Ruane, A. C., Skea, J., Shukla, P. R., Slade, R., Slangen, A., Sokona, Y., Sörensson, A. A., Tignor, M., Van Vuuren, D., Wei, Y.-M., Winkler, H., Zhai, P., Zommers, Z., Hourcade, J.-C., Johnson, F. X., Pachauri, S., Simpson, N. P., Singh, C., Thomas, A., Totin, E., Arias, P., Bustamante, M., Elgizouli, I., Flato, G., Howden, M., Méndez-Vallejo, C., Pereira, J. J., Pichs-Madruga, R., Rose, S. K., Saheb, Y., Sánchez Rodríguez, R., Ürgé-Vorsatz, D., Xiao, C., Yassaa, N., Alegría, A., Armour, K., Bednar-Friedl, B.,  
810 Blok, K., Cissé, G., Dentener, F., Eriksen, S., Fischer, E., Garner, G., Guivarch, C., Haasnoot, M., Hansen, G., Hauser, M., Hawkins, E., Hermans, T., Kopp, R., Leprince-Ringuet, N., Lewis, J., Ley, D., Ludden, C., Niamir, L., Nicholls, Z., Some, S., Szopa, S., Trewin, B., Van Der Wijst, K.-I., Winter, G., Witting, M., Birt, A., Ha, M., et al.: IPCC, 2023: Climate Change



- 2023: Synthesis Report. Contribution of Working Groups I, II and III to the Sixth Assessment Report of the Intergovernmental Panel on Climate Change [Core Writing Team, H. Lee and J. Romero (eds.)]. IPCC, Geneva, Switzerland., Intergovernmental Panel on Climate Change (IPCC), <https://doi.org/10.59327/IPCC/AR6-9789291691647>, 2023.
- 815 Cannon, A. J.: Multivariate quantile mapping bias correction: an N-dimensional probability density function transform for climate model simulations of multiple variables, *Clim Dyn*, 50, 31–49, <https://doi.org/10.1007/s00382-017-3580-6>, 2018.
- Chen, J., Arsenault, R., Brissette, F. P., and Zhang, S.: Climate Change Impact Studies: Should We Bias Correct Climate Model Outputs or Post-Process Impact Model Outputs?, *Water Resources Research*, 57, e2020WR028638, <https://doi.org/10.1029/2020WR028638>, 2021.
- 820 2015 Land Cover of North America at 30 meters: <http://www.cec.org/north-american-environmental-atlas/land-cover-30m-2015-landsat-and-rapideye/>, last access: 1 December 2023.
- Conrad, O., Bechtel, B., Bock, M., Dietrich, H., Fischer, E., Gerlitz, L., Wehberg, J., Wichmann, V., and Böhner, J.: System for Automated Geoscientific Analyses (SAGA) v. 2.1.4, *Geoscientific Model Development*, 8, 1991–2007, <https://doi.org/10.5194/gmd-8-1991-2015>, 2015.
- 825 Devia, G. K., Ganasri, B. P., and Dwarakish, G. S.: A Review on Hydrological Models, *Aquatic Procedia*, 4, 1001–1007, <https://doi.org/10.1016/j.aqpro.2015.02.126>, 2015.
- Estrada, F., Kim, D., and Perron, P.: Spatial variations in the warming trend and the transition to more severe weather in midlatitudes, *Sci Rep*, 11, 145, <https://doi.org/10.1038/s41598-020-80701-7>, 2021.
- 830 Farjad, B., Gupta, A., and Marceau, D. J.: Annual and Seasonal Variations of Hydrological Processes Under Climate Change Scenarios in Two Sub-Catchments of a Complex Watershed, *Water Resour Manage*, 30, 2851–2865, <https://doi.org/10.1007/s11269-016-1329-3>, 2016.
- Förster, K., Meißl, G., Marke, T., Pohl, S., Garvelmann, J., Schulla, J., and Strasser, U.: A new snow-vegetation interaction extension for the Water Balance Simulation Model (WaSiM), 2620, 2017.
- 835 Förster, K., Garvelmann, J., Meißl, G., and Strasser, U.: Modelling forest snow processes with a new version of WaSiM, *Hydrological Sciences Journal*, 63, 1540–1557, <https://doi.org/10.1080/02626667.2018.1518626>, 2018.
- van Genuchten, M. Th.: A Closed-form Equation for Predicting the Hydraulic Conductivity of Unsaturated Soils, *Soil Science Society of America Journal*, 44, 892–898, <https://doi.org/10.2136/sssaj1980.03615995004400050002x>, 1980.
- 840 Hersbach, H., Bell, B., Berrisford, P., Hirahara, S., Horányi, A., Muñoz-Sabater, J., Nicolas, J., Peubey, C., Radu, R., Schepers, D., Simmons, A., Soci, C., Abdalla, S., Abellan, X., Balsamo, G., Bechtold, P., Biavati, G., Bidlot, J., Bonavita, M., De Chiara, G., Dahlgren, P., Dee, D., Diamantakis, M., Dragani, R., Flemming, J., Forbes, R., Fuentes, M., Geer, A., Haimberger, L., Healy, S., Hogan, R. J., Hólm, E., Janisková, M., Keeley, S., Laloyaux, P., Lopez, P., Lupu, C., Radnoti, G., de Rosnay, P., Rozum, I., Vamborg, F., Villaume, S., and Thépaut, J.-N.: The ERA5 global reanalysis, *Quarterly Journal of the Royal Meteorological Society*, 146, 1999–2049, <https://doi.org/10.1002/qj.3803>, 2020.
- 845





- Jakob Themeßl, M., Gobiet, A., and Leuprecht, A.: Empirical-statistical downscaling and error correction of daily precipitation from regional climate models, *International Journal of Climatology*, 31, 1530–1544, <https://doi.org/10.1002/joc.2168>, 2011.
- Jasper, K., Calanca, P., and Fuhrer, J.: Changes in summertime soil water patterns in complex terrain due to climatic change, *Journal of Hydrology*, 327, 550–563, <https://doi.org/10.1016/j.jhydrol.2005.11.061>, 2006.
- 850 Kling, H., Fuchs, M., and Paulin, M.: Runoff conditions in the upper Danube basin under an ensemble of climate change scenarios, *Journal of Hydrology*, 424–425, 264–277, <https://doi.org/10.1016/j.jhydrol.2012.01.011>, 2012.
- Kour, R., Patel, N., and Krishna, A. P.: Climate and hydrological models to assess the impact of climate change on hydrological regime: a review, *Arab J Geosci*, 9, 544, <https://doi.org/10.1007/s12517-016-2561-0>, 2016.
- 855 Latifovic, R., Homer, C., Ressler, R., Pouliot, D. A., Hossain, S., Colditz, R., Olthof, I., Chandra, G., and Victoria, A.: North American Land Change Monitoring System, *Remote Sensing of Land Use and Land Cover: Principles and Applications*, 303–324, <https://doi.org/10.1201/b11964-24>, 2012.
- Lee, M.-H., Lu, M., Im, E.-S., and Bae, D.-H.: Added value of dynamical downscaling for hydrological projections in the Chungju Basin, Korea, *International Journal of Climatology*, 39, 516–531, <https://doi.org/10.1002/joc.5825>, 2019.
- 860 Lucas-Picher, P., Lachance-Cloutier, S., Arsenault, R., Poulin, A., Ricard, S., Turcotte, R., and Brissette, F.: Will Evolving Climate Conditions Increase the Risk of Floods of the Large U.S.-Canada Transboundary Richelieu River Basin?, *JAWRA Journal of the American Water Resources Association*, 57, 32–56, <https://doi.org/10.1111/1752-1688.12891>, 2021.
- Ludwig, R., May, I., Turcotte, R., Vescovi, L., Braun, M., Cyr, J.-F., Fortin, L.-G., Chaumont, D., Biner, S., Chartier, I., Caya, D., and Mauser, W.: The role of hydrological model complexity and uncertainty in climate change impact assessment, *Advances in Geosciences*, 21, 63–71, <https://doi.org/10.5194/adgeo-21-63-2009>, 2009.
- 865 Mei, Y., Mai, J., Do, H. X., Gronewold, A., Reeves, H., Eberts, S., Niswonger, R., Regan, R. S., and Hunt, R. J.: Can Hydrological Models Benefit From Using Global Soil Moisture, Evapotranspiration, and Runoff Products as Calibration Targets?, *Water Resources Research*, 59, e2022WR032064, <https://doi.org/10.1029/2022WR032064>, 2023.
- Milly, P. C. D., Dunne, K. A., and Vecchia, A. V.: Global pattern of trends in streamflow and water availability in a changing climate, *Nature*, 438, 347–350, <https://doi.org/10.1038/nature04312>, 2005.
- 870 Ministère du Développement durable, de l'Environnement et de la Lutte contre les changements climatiques: *Hydroclimatic Atlas of Southern Québec (3rd ed.)*, available at: <https://www.cehq.gouv.qc.ca/atlas-hydroclimatique/index-en.htm>, last access: 30 November 2023.
- Ministère des Ressources Naturelles et des Forêts: *SIIGSOL-100m - Carte des propriétés du sol, Données Québec, 2022*.
- 875 Minville, M., Brissette, F., and Leconte, R.: Uncertainty of the impact of climate change on the hydrology of a nordic watershed, *Journal of Hydrology*, 358, 70–83, <https://doi.org/10.1016/j.jhydrol.2008.05.033>, 2008.
- Mpelasoka, F. S. and Chiew, F. H. S.: Influence of Rainfall Scenario Construction Methods on Runoff Projections, <https://doi.org/10.1175/2009JHM1045.1>, 2009.



- Natkhin, M., Steidl, J., Dietrich, O., Dannowski, R., and Lischeid, G.: Differentiating between climate effects and forest growth dynamics effects on decreasing groundwater recharge in a lowland region in Northeast Germany, *Journal of Hydrology*, 448–449, 245–254, <https://doi.org/10.1016/j.jhydrol.2012.05.005>, 2012.
- Nolin, A. F., Girardin, M. P., Adamowski, J. F., Barzegar, R., Boucher, M.-A., Tardif, J. C., and Bergeron, Y.: Observed and projected trends in spring flood discharges for the Upper Harricana River, eastern boreal Canada, *Journal of Hydrology: Regional Studies*, 48, 101462, <https://doi.org/10.1016/j.ejrh.2023.101462>, 2023.
- 885 O’Neill, B. C., Tebaldi, C., van Vuuren, D. P., Eyring, V., Friedlingstein, P., Hurtt, G., Knutti, R., Kriegler, E., Lamarque, J.-F., Lowe, J., Meehl, G. A., Moss, R., Riahi, K., and Sanderson, B. M.: The Scenario Model Intercomparison Project (ScenarioMIP) for CMIP6, *Geoscientific Model Development*, 9, 3461–3482, <https://doi.org/10.5194/gmd-9-3461-2016>, 2016.
- Piani, C., Haerter, J. O., and Coppola, E.: Statistical bias correction for daily precipitation in regional climate models over Europe, *Theor Appl Climatol*, 99, 187–192, <https://doi.org/10.1007/s00704-009-0134-9>, 2010.
- 890 Poulin, A., Brissette, F., Leconte, R., Arsenault, R., and Malo, J.-S.: Uncertainty of hydrological modelling in climate change impact studies in a Canadian, snow-dominated river basin, *Journal of Hydrology*, 409, 626–636, <https://doi.org/10.1016/j.jhydrol.2011.08.057>, 2011.
- Ricard, S., Sylvain, J.-D., and Anctil, F.: Exploring an Alternative Configuration of the Hydroclimatic Modeling Chain, Based on the Notion of Asynchronous Objective Functions, *Water*, 11, 2012, <https://doi.org/10.3390/w11102012>, 2019.
- 895 Ricard, S., Sylvain, J.-D., and Anctil, F.: Asynchronous Hydroclimatic Modeling for the Construction of Physically Based Streamflow Projections in a Context of Observation Scarcity, *Frontiers in Earth Science*, 8, 2020.
- Ricard, S., Lucas-Picher, P., Thibault, A., and Anctil, F.: Producing reliable hydrologic scenarios from raw climate model outputs without resorting to meteorological observations, *Hydrology and Earth System Sciences*, 27, 2375–2395, <https://doi.org/10.5194/hess-27-2375-2023>, 2023.
- 900 Richards, L. A.: CAPILLARY CONDUCTION OF LIQUIDS THROUGH POROUS MEDIUMS, *Physics*, 1, 318–333, <https://doi.org/10.1063/1.1745010>, 1931.
- WaSiM-ETH Documentation: [http://www.wasim.ch/en/products/wasim\\_description.htm](http://www.wasim.ch/en/products/wasim_description.htm), last access: 30 November 2023.
- Sivakumar, B.: Global climate change and its impacts on water resources planning and management: assessment and challenges, *Stoch Environ Res Risk Assess*, 25, 583–600, <https://doi.org/10.1007/s00477-010-0423-y>, 2011.
- 905 Soil Survey Division Staff: *Soil Survey Manual*, Handbook 18, U.S. Department of Agriculture, Soil Conservation Service, 2017.
- Sylvain, J.-D., Anctil, F., and Thiffault, E.: Using bias correction and ensemble modelling for predictive mapping and related uncertainty: A case study in digital soil mapping, *Geoderma*, 403, 1–29, <https://doi.org/10.1016/j.geoderma.2021.115153>, 2021.
- 910



- T. W. Chu and A. Shirmohammadi: EVALUATION OF THE SWAT MODELS HYDROLOGY COMPONENT IN THE  
PIEDMONT PHYSIOGRAPHIC REGION OF MARYLAND, *Transactions of the ASAE*, 47, 1057–1073,  
<https://doi.org/10.13031/2013.16579>, 2004.
- 915 Talbot, F., Sylvain, J.-D., Drolet, G., Poulin, A., and Arsenault, R.: Enhancing physically based and distributed hydrological  
model calibration through internal state variable constraints, *Hydrology and Earth System Sciences*, [under review], initial  
submission: 24 September 2024a.
- Talbot, F., Sylvain, J.-D., Drolet, G., Poulin, A., and Arsenault, R.: Assessing hydroclimatic impacts of climate change in  
snowy catchments using a physically based hydrological model, *Hydrology and Earth System Sciences*, [under review],  
initial submission: 27 September 2024b.
- 920 Talbot, F., Ricard, S., Sylvain, J.-D., Drolet, G., Poulin, A., and Arsenault, R.: HESS paper data - Wasim Semi-  
Asynchronous climate change impact modelling, <https://doi.org/10.17605/OSF.IO/N87EY>, 2024c.
- Tarek, M., Brissette, F. P., and Arsenault, R.: Evaluation of the ERA5 reanalysis as a potential reference dataset for  
hydrological modelling over North America, *Hydrology and Earth System Sciences*, 24, 2527–2544,  
<https://doi.org/10.5194/hess-24-2527-2020>, 2020.
- 925 Tarek, M., Brissette, F., and Arsenault, R.: Uncertainty of gridded precipitation and temperature reference datasets in climate  
change impact studies, *Hydrology and Earth System Sciences*, 25, 3331–3350, <https://doi.org/10.5194/hess-25-3331-2021>,  
2021.
- Tolson, B. A. and Shoemaker, C. A.: Dynamically dimensioned search algorithm for computationally efficient watershed  
model calibration, *Water Resources Research*, 43, <https://doi.org/10.1029/2005WR004723>, 2007.
- 930 Valencia Giraldo, M. del C., Ricard, S., and Ancil, F.: Assessment of the Potential Hydrological Impacts of Climate Change  
in Quebec—Canada, a Refined Neutral Approach, *Water*, 15, 584, <https://doi.org/10.3390/w15030584>, 2023.
- Yassin, F., Razavi, S., Wheeler, H., Saprizo-Azuri, G., Davison, B., and Pietroniro, A.: Enhanced identification of a  
hydrologic model using streamflow and satellite water storage data: A multicriteria sensitivity analysis and optimization  
approach, *Hydrological Processes*, 31, 3320–3333, <https://doi.org/10.1002/hyp.11267>, 2017.

935